clone, compared with monotransfection of the wild-type HBV/G (Fig. 2a). The intracellular expression of core protein in the cell lysates and the expression of HBsAg in the culture supernatant were also enhanced by the co-transfection with both HBV/A2 and HBV/G clones (Fig. 2b and 2c). Removing the 36-nt insertion from the wild-type HBV/G genome resulted in a significant reduction in viral replication and core protein expression compared with the wild-type HBV/G clone. These results are in agreement with the observations of a previous study [13].

The core protein of HBV/A2 is essential for efficient replication of HBV/G

To determine how HBV/A2 rescues HBV/G replication during co-transfection, we constructed four HBV/A2 recombinant plasmids that selectively expressed one of the four viral proteins, whereas translation of the other three was prevented by the introduction of stop codons (Fig. 1a). All of these plasmids were prevented from coding for the viral pregenomic RNA containing the 'packaging-negative' mutation in the ε signal loop to abrogate encapsidation (see Materials and methods). Huh7 cells were co-transfected with the wild-type HBV/G clone and one of the four plasmids expressing a single viral protein. According to Southern blot analysis, the expression of intracellular HBV DNA was greatly increased when HBV/G was co-transfected with HBV/A2-core compared with the other three expression plasmids or the experimental control (pUC19 or HBV/A2-N) (Fig. 3a). The intracellular expression of core protein in the cell lysates was also the highest when HBV/G was co-transfected with HBV/A2-core (Fig. 3b). The expression of HBsAg in the culture supernatant was only increased when HBV/G was co-transfected with the HBV/A2-S plasmid (Fig. 3c). These results indicated that the core protein translated from the HBV/A2 recombinant plasmid can enhance HBV/G replication.

The core protein of HBV/A2 is more effective than those of HBV/C and HBV/G at promoting HBV/G replication

To compare the effects of genotype on the ability of the core protein to increase HBV/G replication in co-transfection experiments, we generated three genotype-specific core protein expression constructs (HBV/G, HBV/A2 and HBV/C) driven by the CMV promoter, which produced core protein in the absence of a preceding ε signal (Fig. 1c). Huh7 cells were co-transfected with HBV/G and one of the three core protein expression vectors. Southern blot analysis showed that the level of intracellular HBV DNA was highest during co-transfection with CMV-HBV/A2/core, followed by CMV-HBV/G/core, and was lowest for CMV-HBV/C/core (Fig. 4a), although the expression of core protein in the cell lysates was the highest during co-transfection with CMV-HBV/C/core, followed by CMV-HBV/G/core, and CMV-HBV/A2/core (Fig. 4b). As anticipated, there was no difference in the expression levels of HBsAg in any co-transfection experiment (Fig. 4c).

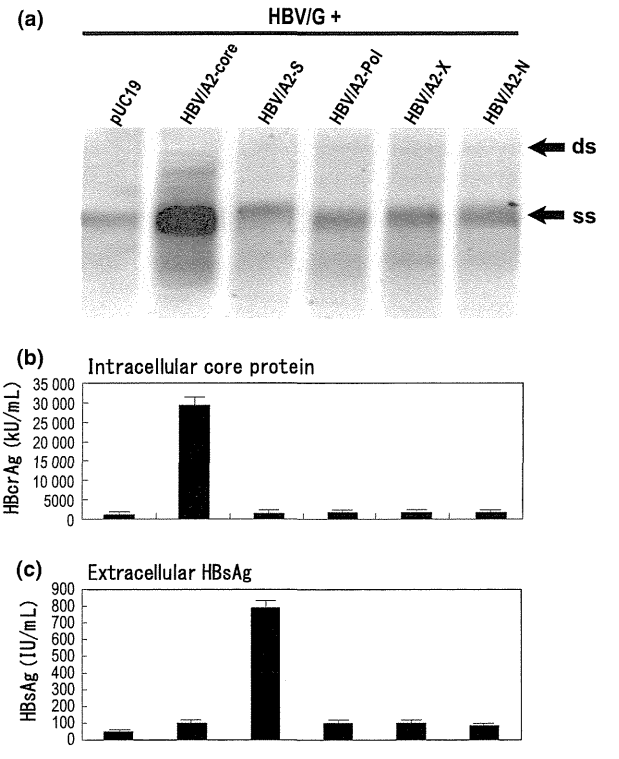

Fig. 3 (a) Southern blot analysis for replication competence of HBV/G clones co-transfected with each of the four HBV/A2 recombinant plasmids: HBV/A2-S, HBV/A2-core, HBV/A2-pol and HBV/A2-X selectively expressing only one of the four viral proteins (large surface, precore/core, polymerase or X protein, respectively). The 'HBV/A2-N' contained all the six mutations to be used as an experimental control. All of the above HBV/A2 recombinant plasmids had the 'packaging-negative' mutation in the ε signal to abrogate encapsidation. (b) Intracellular expression of core protein was measured as described in Fig. 2b. (c) The expression of HBsAg in the culture supernatant was detected as described in Fig. 2c.

A comparison of viral replication among HBV/G and recombinant HBV/G clones

To examine the effects of genetic recombination and the roles of the core promoter, precore and core genomic regions in the interaction of HBV/G and HBV/A2 during co-transfection, we employed three HBV/G and HBV/A2 chimaeric replicating constructs (see Materials and methods), which are shown in Fig. 1c. After the transfection experiment, Southern blot analysis of cell lysates indicated an abundant level of DNA expression in HBV/G/A2-CP/core–transfected cells compared with those in the cells transfected with HBV/G-wild type, HBV/G/A2-CP and HBV/G/A2-core (Fig. 5a). As shown in Fig. 5b, the highest

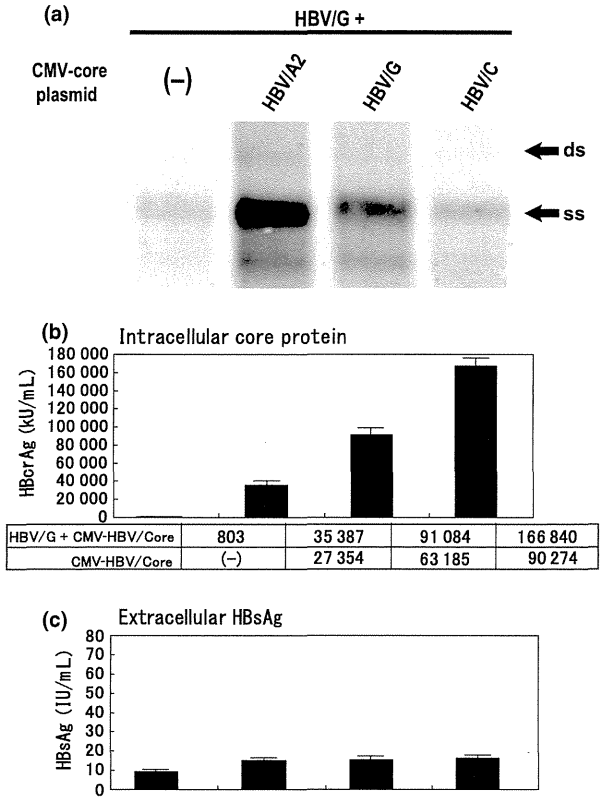

Fig. 4 (a) Southern blot analysis for the expression of intracellular HBV/G DNA during co-transfection with the three core protein expression constructs for each genotype (HBV/G, HBV/A2 and HBV/C) driven by the CMV promoter, which produced core protein in the absence of a preceding ε signal. (b) Intracellular expression of core protein. (c) The expression of HBsAg in the culture supernatant.

levels of core protein (HBcrAg) expression were observed for the HBV/G/A2-CP and HBV/G/A2-CP/core-transfected cultures, which was in sharp contrast with the low levels observed in the HBV/G/A2-core and the wild-type HBV/G cultures. The discrepancy between viral replication and core production of the HBV/G/A2-CP clone might indicate insufficient virion assembly. Figure 5c shows the HBeAg levels measured in culture supernatants. The expression of HBeAg was the highest in the HBV/G/A2-CP/core culture distantly followed by that in the HBV/G/A2-core culture. The HBV/G/A2-CP and wild-type HBV/G clones expressed HBeAg protein at levels close to or below the level of detection. Nevertheless, a high HBcrAg titre was detected in the cell lysate of the HBV/G/A2-CP clone, although its DNA level was as low as that of the wild-type HBV/G clone (Fig. 5a). These results indicated that low replication of HBV/G might be explained by low synthesis of HBV/G core protein due to weak core promoter activity or dysfunction, as well as insufficient virion assembly due to the larger core protein of HBV/G (12-aa unique insertion).

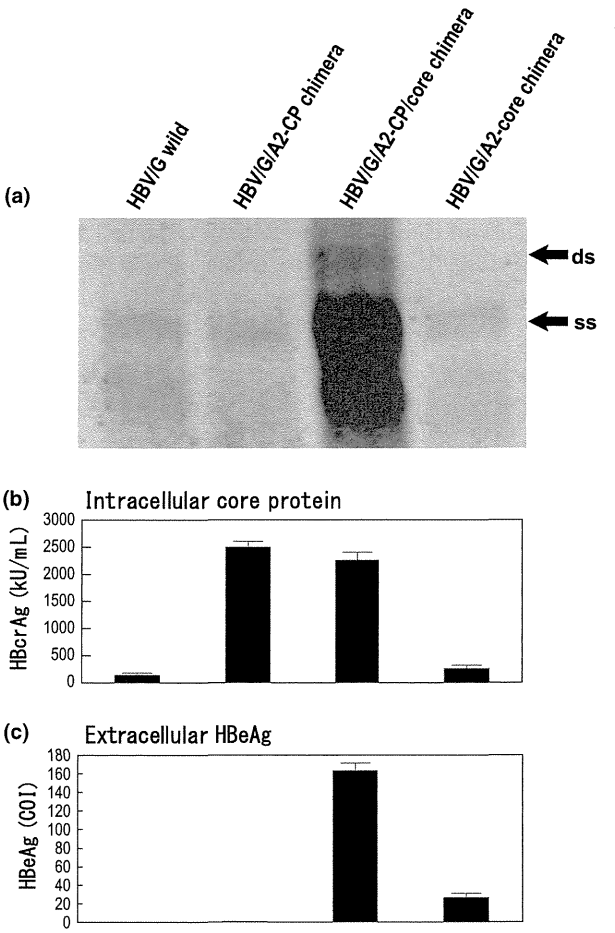

Fig. 5 (a) Southern blot analysis for HBV replication among HBV/G and three chimeric replicating constructs created by recombination of different genomic sections of HBV/G and HBV/A2 (see Materials and methods). The 'HBV/G/A2-CP' clone was a HBV/G-based construct in which the fragment containing the core promoter (CP) region but not the precore or core was replaced by the corresponding sequence from HBV/A2. The 'HBV/G/A2-Core' clone was an HBV/G-based construct in which the section of the precore and core region was replaced with that of HBV/A2. For the 'HBV/G/A2-CP/core' clone, the CP, precore and core region of HBV/G were replaced with that of HBV/A2. (b) Intracellular expression of core protein. (c) Extracellular expression of HBeAg levels detected by a commercial chemiluminescent enzyme immunoassay (mean and standard deviation, $n = 3$).

Dane particles produced by HBV/G during co-transfection with HBV/A2 were packed in HBV/A2 protein

To investigate the effects of HBV/A2 core protein during HBV/G viral assembly, we tried to define whether the Dane particles in B Huh7 cells that had been co-transfected with wild-type HBV/G and the CMV-HBV/A2-core plasmid

(source of the Fig. 4 lane 2) contained HBV/A2 or HBV/G core protein. To extract the Dane particles, we employed ultracentrifugation of the culture media through a 10–60% (w/w) sucrose density gradient followed by immunoprecipitation using anti-HBs-coated magnetic beads. We thereby extracted Dane particles, which were then analysed using Western blotting. The obtained fractions were tested for HBcrAg, HBsAg and HBV DNA (Fig. 6a). HBcrAg appeared in the high-density fractions, and its levels peaked in the same fraction (fraction 22) as HBV DNA. As reported previously, the fraction in which the levels of HBV DNA and HBcrAg peaked contained Dane particles [22]. To eliminate contamination of the Dane particles with 'naked' core particles or core protein, they were specifically retrieved from sucrose high-density fraction 22 by means of immunoprecipitation using anti-HBs-coated magnetic beads. The media supernatant obtained from the culture of cells that had been subjected to CMV-HBV/A2/core clone monotransfection was also subjected to sucrose gradient ultracentrifugation using the same protocol. Sucrose high-density fraction 22, in which the HBcrAg concentration peaked, presumably contained 'naked' core particles or core protein (Fig. 6b). This fraction was collected and processed in the same manner via anti-HBs-coated magnetic bead separation and was used as negative control for this procedure (Fig. 6c, lane 4). To discriminate between HBV/G and HBV/A2 core proteins on Western blot analysis probed with anti-HBc antibody, we employed cell lysates produced from cells that had been transfected with the wild-type HBV/G clone and those produced with the HBV/A2 clone as controls. As can be seen on the Western blotting image (Fig. 6c), HBV/G-transfected cells (lane 1) produced larger proteins than the HBV/A2-transfected cells (lane 2), which can be explained by the 12-aa insertion in the core protein of HBV/G coded by its 36-nt unique insertion. Interestingly, the most saturated band associated with the Dane particles produced by HBV/G that had been co-transfected with CMV-HBV/A2/core (lane 3) was the same size as that for HBV/A2, suggesting that HBV/G competitively produces Dane particles consisting of HBV/A2 core protein during virion assembly.

DISCUSSION

HBV/G was first isolated in 2000 in France and the USA and was later found in Thailand, Japan and Mexico, indicating its global dissemination and association with specific risk groups, such as injection drug users (IDU) and men who had sex with men (MSM) [25]. Studies have also demonstrated that throughout the world, HBV/G strains possess unprecedented genetic homology and are mainly detected during co-infection with another genotype that is endemic in the area. Further studies have suggested that genotype G represents a 'replication-defective' variant of HBV that requires co-infection with another genotype to establish a persistent infection. We and others have reported *in vitro* and *in vivo* experimental evidence of this HBV/G dependence [13–15]. The unique 36-nt insertion within core coding region increases core protein level and genome replication in genotype G but impairs replication, not core protein expression, in other genotypes [14]. These results strongly suggest the 36-nt/12-aa insertion has pleiotropic effects on core protein expression, genome replication and virion secretion [14]. To obtain clues about the mechanism by which genotype G works in combination with genotype A to effect its replication, we performed co-transfection experiments using Huh7 cells.

Using HBV/A2 viral proteins expressing plasmids, we determined that a HBV/A2 plasmid that selectively expressed core protein was capable of increasing the replication of the wild-type HBV/G (Fig. 3a). The replication of HBV/G during co-transfection was not affected by other viral elements of HBV/A2 because of the presence of the 'packaging-negative mutation' in the epsilon-coding region and stop codons preventing the translation of the other three viral proteins (the polymerase, surface and X proteins). The specific role of the core protein was further confirmed in experiments with CMV promoter–driven core expressing constructs, in which the core protein alone enhanced HBV/G replication in the absence of HBV pregenomic RNA. Interestingly, co-transfection of HBV/G with the CMV-HBV/A2/core expression construct produced the highest levels of intracellular DNA, even though this combination produced the lowest intracellular core protein level, compared with the CMV-core constructs of the other two genotypes (HBV/G and HBV/C) (Figs 4a,b). The replication of HBV/G was the highest during co-transfection with the CMV-HBV/A2/core expression construct, which agreed with the results of experiments using other genotype (HBV/D, HBV/B1) CMV-core constructs (data not shown). Thus, the core protein of HBV/A2 was confirmed to play an important role in upregulating HBV/G replication and performed this task more efficiently than the other genotypes. These experimental results might explain why HBV/A is the genotype that is most frequently found in co-infections with HBV/G [12,26].

Moreover, HBV/G core protein overexpression achieved by the co-transfection of HBV/G with CMV-HBV/G/core did not enhance replication, suggesting that HBV/G core protein is functionally defective; that is, results in insufficient viral packaging. To investigate the functional defect in the HBV/G core protein, we exchanged the core gene of the wild-type HBV/G for the corresponding gene of HBV/A2 (HBV/G/A2-core); the introduction of the HBV/A2 core promoter together with core coding region into the HBV/G genome (HBV/G/A2-CP/core) significantly enhanced replication. However, the replication of the recombinant construct (HBV/A2 core coding region; HBV/G/A2-core) did not differ from that of the wild-type HBV/G, suggesting that the replacement of HBV/G/A2-core alone was not

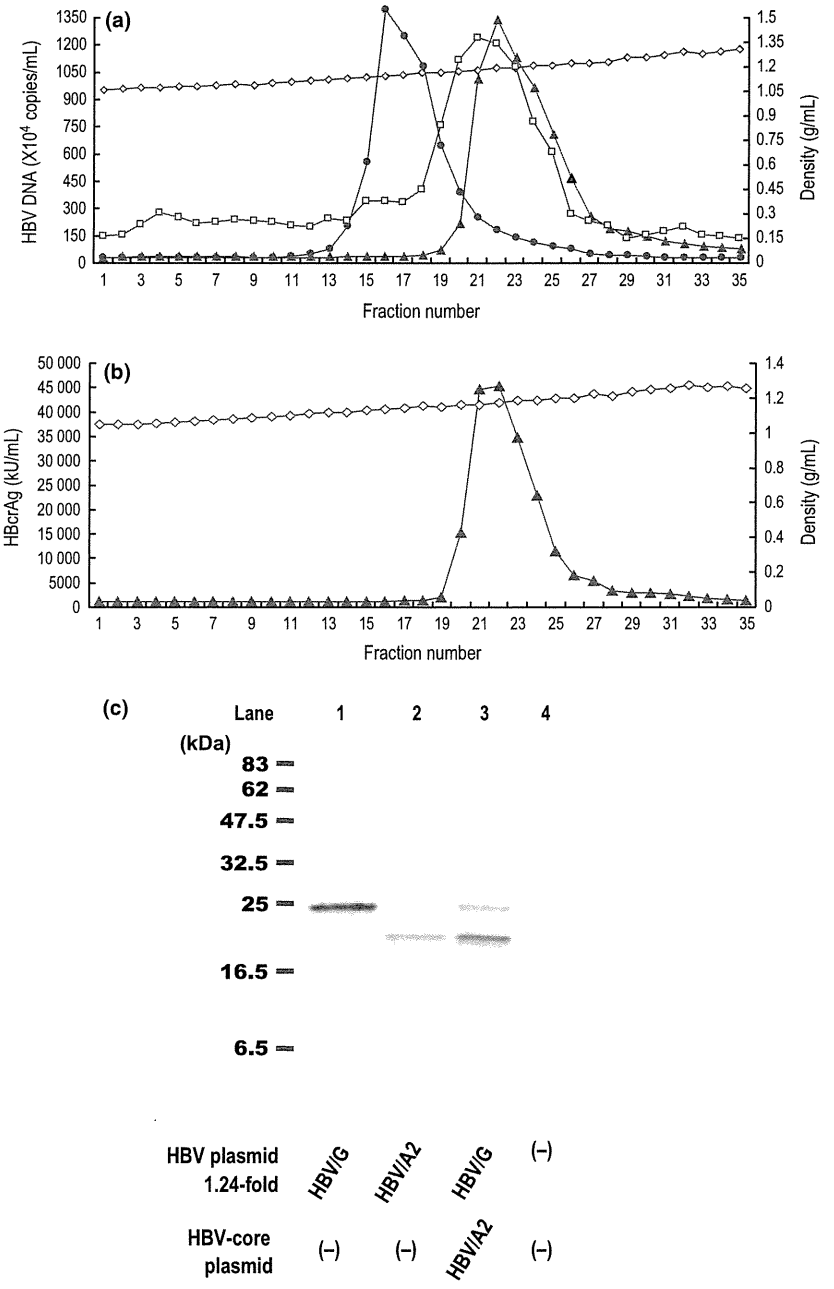

Fig. 6 (a) Sucrose gradient analysis of the culture media of Huh7 cells that had been co-transfected with wild-type HBV/G and the CMV-HBV/A2-core plasmid. It was subjected to ultracentrifugation through a 10–60% (w/w) sucrose density gradient. Density of each fraction is shown as a line with diamond symbols. Fractions were diluted 10-fold and tested for HBsAg (•) (IU/mL), HBcrAg (▲) (KU/mL) and HBV DNA (□) (10^4 copies/mL). (b) Sucrose gradient analysis of culture supernatant obtained from the cells that were subjected to CMV-HBV/A2/core monotransfection using the same protocol. (c) Western blot analysis for HBV core protein was probed by anti-HBc antibody. HBV/G/core and HBV/A2/core were obtained from cell lysates that were transfected with the wild-type HBV/G clone and the wild-type HBV/A2 clone, respectively. The 'HBV/G + CMV-HBV/A2/core' was obtained from sucrose high-density fraction 22 (Fig. 6a) that had been co-transfected with wild-type HBV/G and the CMV-HBV/A2-core plasmid by means of immunoprecipitation using anti-HBs-coated magnetic beads.

enough for viral replication because the core promoter of HBV/G was not capable of generating sufficient amounts of core protein to enhance HBV replication. As well, an HBV/G/A2-CP construct containing the HBV/A core promoter region in the context of the wild-type HBV/G genome did not enhance replication, even though its core protein

production was significantly increased (Figs 5a,b). Although it was previously reported that the 36-nt insertion of the HBV/G core gene was required for both efficient core protein expression and HBV/G replication [13], in this study, the discrepancy between viral replication and core production of the HBV/G/A2-CP clone might indicate insufficient virion assembly due to the larger core protein of HBV/G (12-aa unique insertion). *Trans*-complementation experiments carried out by Gutelius *et al.* [14] demonstrated an association between enhanced core protein level and reduced replication capacity only when the core and polymerase proteins are expressed from the same RNA template. Thus, it was indicated that HBV/G itself could not replicate sufficiently due to a defect in its core protein and/or the core promoter of HBV/G.

Finally, we investigated whether HBV/G utilises the core protein of HBV/A2 for virion packaging. Dane particles obtained from the culture supernatants of cells that had been co-transfected with HBV/G and CMV-HBV/A2/core were assessed by Western blotting, and it was found that the Dane particles of HBV/G contained HBV/A core proteins. Thus, it was implied that HBV/G replication is enhanced by the core protein of HBV/A because it is more suitable for virion packaging than its own core protein, suggesting that the core protein of HBV/A is a key element enhancing the replication of HBV/G during co-infection. Interestingly, our experiments demonstrated that there were large differences in core protein expression among the CMV-core constructs of different genotypes, despite the fact that all of the CMV-core constructs had the same CMV promoter (Fig. 4b). In a previous report, it was speculated that the core protein binds to its own mRNA to influence protein translation [13]. For example, dihydrofolate reductase protein has been found to downregulate its own translation by binding to cognate mRNA [27,28]. Therefore, we predict that the core protein of HBV/A2 enhances HBV/G replication by affecting viral promoters or transcription in addition to its role in virion packaging.

In conclusion, enhanced replication of HBV/G requires the HBV/A2 core protein during co-infection with HBV/A2. Our findings provide a possible explanation that the core protein of HBV/A2 is more suitable for virion packaging rather than that of HBV/G, and the replication of HBV/G occurs at a very low level, which may be due to defects in its core protein functions and/or core promoter activity. Further experiments are warranted to clarify the detailed roles of the enhanced HBV/G replication by co-infection with the other genotype and the clinical manifestation of HBV/G infection.

ACKNOWLEDGEMENTS

This study was supported, in part, by a grant-in-aid from the Ministry of Health, Labour and Welfare of Japan and a grant-in-aid from the Ministry of Education, Culture, Sports, Science and Technology. We thank Ms H. Naganuma of Nagoya City University Graduate School of Medical Sciences, Nagoya, Japan, for doing serological assays.

CONFLICT OF INTEREST STATEMENT

None declared.

REFERENCES

1 Kao JH, Chen DS. Global control of hepatitis B virus infection. *Lancet Infect Dis* 2002; 2(7): 395–403. Epub 2002/07/20.
2 Kim BK, Revill PA, Ahn SH. HBV genotypes: relevance to natural history, pathogenesis and treatment of chronic hepatitis B. *Antivir Ther* 2011; 16(8): 1169–1186. Epub 2011/12/14.
3 Okamoto H, Tsuda F, Sakugawa H, Sastrosoewignjo RI, Imai M, Miyakawa Y *et al.* Typing hepatitis B virus by homology in nucleotide sequence: comparison of surface antigen subtypes. *J Gen Virol* 1988; 69 (Pt 10): 2575–2583. Epub 1988/10/01.
4 Norder H, Courouce AM, Magnius LO. Complete genomes, phylogenetic relatedness, and structural proteins of six strains of the hepatitis B virus, four of which represent two new genotypes. *Virology* 1994; 198(2): 489–503. Epub 1994/02/01.
5 Orito E, Ichida T, Sakugawa H, Sata M, Horiike N, Hino K *et al.* Geographic distribution of hepatitis B virus (HBV) genotype in patients with chronic HBV infection in Japan. *Hepatology* 2001; 34(3): 590–594. Epub 2001/08/30.
6 Stuyver L, De Gendt S, Van Geyt C, Zoulim F, Fried M, Schinazi RF *et al.* A new genotype of hepatitis B virus: complete genome and phylogenetic relatedness. *J Gen Virol* 2000; 81(Pt 1): 67–74. Epub 2000/01/21.
7 Kato H, Orito E, Gish RG, Bzowej N, Newsom M, Sugauchi F *et al.* Hepatitis B e antigen in sera from individuals infected with hepatitis B virus of genotype G. *Hepatology* 2002; 35(4): 922–929. Epub 2002/03/27.
8 Osiowy C, Gordon D, Borlang J, Giles E, Villeneuve JP. Hepatitis B virus genotype G epidemiology and co-infection with genotype A in Canada. *J Gen Virol* 2008; 89(Pt 12): 3009–3015. Epub 2008/11/15.
9 Suwannakarn K, Tangkijvanich P, Theamboonlers A, Abe K, Poovorawan Y. A novel recombinant of hepatitis B virus genotypes G and C isolated from a Thai patient with hepatocellular carcinoma. *J Gen Virol* 2005; 86(Pt 11): 3027–3030. Epub 2005/10/18.
10 Sanchez LV, Tanaka Y, Maldonado M, Mizokami M, Panduro A. Difference of hepatitis B virus genotype distribution in two groups of Mexican

patients with different risk factors. High prevalence of genotype H and G. *Intervirology* 2007; 50(1): 9–15. Epub 2006/12/14.

11 Tanaka Y, Sanchez LV, Sugiyama M, Sakamoto T, Kurbanov F, Tatematsu K *et al.* Characteristics of hepatitis B virus genotype G coinfected with genotype H in chimeric mice carrying human hepatocytes. *Virology* 2008; 376(2): 408–415. Epub 2008/05/14.

12 Kato H, Orito E, Gish RG, Sugauchi F, Suzuki S, Ueda R *et al.* Characteristics of hepatitis B virus isolates of genotype G and their phylogenetic differences from the other six genotypes (A through F). *J Virol* 2002; 76(12): 6131–6137. Epub 2002/05/22.

13 Li K, Zoulim F, Pichoud C, Kwei K, Villet S, Wands J *et al.* Critical role of the 36-nucleotide insertion in hepatitis B virus genotype G in core protein expression, genome replication, and virion secretion. *J Virol* 2007; 81(17): 9202–9215. Epub 2007/06/15.

14 Gutelius D, Li J, Wands J, Tong S. Characterization of the pleiotropic effects of the genotype G-specific 36-nucleotide insertion in the context of other hepatitis B virus genotypes. *J Virol* 2011; 85(24): 13278–13289. Epub 2011/10/14.

15 Sugiyama M, Tanaka Y, Sakamoto T, Maruyama I, Shimada T, Takahashi S *et al.* Early dynamics of hepatitis B virus in chimeric mice carrying human hepatocytes monoinfected or coinfected with genotype G. *Hepatology* 2007; 45(4): 929–937. Epub 2007/03/30.

16 Lacombe K, Massari V, Girard PM, Serfaty L, Gozlan J, Pialoux G *et al.* Major role of hepatitis B genotypes in liver fibrosis during coinfection with HIV. *AIDS* 2006; 20(3): 419–427. Epub 2006/01/28.

17 Sugiyama M, Tanaka Y, Kato T, Orito E, Ito K, Acharya SK *et al.* Influence of hepatitis B virus genotypes on the intra- and extracellular expression of viral DNA and antigens. *Hepatology* 2006; 44(4): 915–924. Epub 2006/09/29.

18 Bruss V, Ganem D. The role of envelope proteins in hepatitis B virus assembly. *Proc Natl Acad Sci U S A* 1991; 88(3): 1059–1063. Epub 1991/02/01.

19 Tang H, Delgermaa L, Huang F, Oishi N, Liu L, He F *et al.* The transcriptional transactivation function of HBx protein is important for its augmentation role in hepatitis B virus replication. *J Virol* 2005; 79(9): 5548–5556. Epub 2005/04/14.

20 Pollack JR, Ganem D. An RNA stem-loop structure directs hepatitis B virus genomic RNA encapsidation. *J Virol* 1993; 67(6): 3254–3263. Epub 1993/06/01.

21 Ozasa A, Tanaka Y, Orito E, Sugiyama M, Kang JH, Hige S *et al.* Influence of genotypes and precore mutations on fulminant or chronic outcome of acute hepatitis B virus infection. *Hepatology* 2006; 44(2): 326–334. Epub 2006/07/28.

22 Kimura T, Ohno N, Terada N, Rokuhara A, Matsumoto A, Yagi S *et al.* Hepatitis B virus DNA-negative Dane particles lack core protein but contain a 22-kDa precore protein without C-terminal arginine-rich domain. *J Biol Chem* 2005; 280(23): 21713–21719. Epub 2005/04/09.

23 Fujiwara K, Tanaka Y, Paulon E, Orito E, Sugiyama M, Ito K *et al.* Novel type of hepatitis B virus mutation: replacement mutation involving a hepatocyte nuclear factor 1 binding site tandem repeat in chronic hepatitis B virus genotype E. *J Virol* 2005; 79(22): 14404–14410. Epub 2005/10/29.

24 Orchard S, Martens L, Tasman J, Binz PA, Albar JP, Hermjakob H. 6th HUPO Annual World Congress – Proteomics Standards Initiative Workshop 6–10 October 2007, Seoul, Korea. *Proteomics* 2008; 8(7): 1331–1333. Epub 2008/03/05.

25 Kurbanov F, Tanaka Y, Mizokami M. Geographical and genetic diversity of the human hepatitis B virus. *Hepatol Res* 2010; 40(1): 14–30. Epub 2010/02/17.

26 Osiowy C, Giles E. Evaluation of the INNO-LiPA HBV genotyping assay for determination of hepatitis B virus genotype. *J Clin Microbiol* 2003; 41(12): 5473–5477. Epub 2003/12/10.

27 Chu E, Takimoto CH, Voeller D, Grem JL, Allegra CJ. Specific binding of human dihydrofolate reductase protein to dihydrofolate reductase messenger RNA in vitro. *Biochemistry* 1993; 32(18): 4756–4760. Epub 1993/05/11.

28 Ercikan-Abali EA, Banerjee D, Waltham MC, Skacel N, Scotto KW, Bertino JR. Dihydrofolate reductase protein inhibits its own translation by binding to dihydrofolate reductase mRNA sequences within the coding region. *Biochemistry* 1997; 36(40): 12317–12322. Epub 1997/10/07.

SUPPORTING INFORMATION

Additional Supporting Information may be found in the online version of this article:

Data S1. Plasmid construct of HBV/G.

nature medicine

A new cloning and expression system yields and validates TCRs from blood lymphocytes of patients with cancer within 10 days

Eiji Kobayashi[1,4], Eishiro Mizukoshi[2,4], Hiroyuki Kishi[1], Tatsuhiko Ozawa[1], Hiroshi Hamana[1], Terumi Nagai[1], Hidetoshi Nakagawa[2], Aishun Jin[1,3], Shuichi Kaneko[2] & Atsushi Muraguchi[1]

Antigen-specific T cell therapy, or T cell receptor (TCR) gene therapy, is a promising immunotherapy for infectious diseases and cancers. However, a suitable rapid and direct screening system for antigen-specific TCRs is not available. Here, we report an efficient cloning and functional evaluation system to determine the antigen specificity of TCR cDNAs derived from single antigen-specific human T cells within 10 d. Using this system, we cloned and analyzed 380 Epstein-Barr virus–specific TCRs from ten healthy donors with latent Epstein-Barr virus infection and assessed the activity of cytotoxic T lymphocytes (CTLs) carrying these TCRs against antigenic peptide–bearing target cells. We also used this system to clone tumor antigen–specific TCRs from peptide-vaccinated patients with cancer. We obtained 210 tumor-associated antigen–specific TCRs and demonstrated the cytotoxic activity of CTLs carrying these TCRs against peptide-bearing cells. This system may provide a fast and powerful approach for TCR gene therapy for infectious diseases and cancers.

New immunotherapies such as adoptive cell transfer, TCR gene therapy and peptide vaccination have the potential to cure human disease in the future. Rosenberg and his colleagues have reported the adoptive transfer of TCR gene–modified T cells into patients using autologous T cells expressing a TCR recognizing the melanoma-melanocyte differentiation antigen[1,2]. Subsequent clinical trials have targeted antigens such as oncofetal antigen, cancer testis antigen, tissue-specific antigen and overexpressed tumor-associated antigens (TAAs)[3,4]. However, despite its great potential, TCR gene therapy for cancer is still limited to certain tumor antigens and common human leukocyte antigen (HLA) complexes. The conventional approaches for TCR gene cloning involve the establishment of antigen-specific T cell clones, which usually requires several months. Thus, a rapid screening system for antigen-specific TCR genes is needed.

Our group and others have reported single-cell RT-PCR protocols that permit the simultaneous identification of complementarity determining region 3α (CDR3α) and CDR3β transcripts in human[5] and mouse[6] TCRs. However, these protocols cannot retrieve TCRαβ pairs and determine their properties, including antigen specificity and cytotoxicity-inducing activity. In this study, we attempted to establish a direct TCR cloning system that would allow the unbiased analysis of the TCR repertoire, as well as the retrieval of antigen-specific TCRαβ pairs and the characterization of their function for future TCR gene therapy.

RESULTS

Rapid cloning and evaluation of antigen-specific TCRs

We depict the schematic for our rapid cloning and functional assay system, which can obtain TCRαβ cDNA pairs from a single antigen-specific human T cell and confirm their antigen specificity within 10 d (**Fig. 1** and **Supplementary Fig. 1**). This system was designated 'hTEC10' (human TCR efficient cloning within 10 d).

To evaluate the hTEC10 system for analyzing T cells in human disease, we first analyzed Epstein-Barr virus (EBV)-specific $CD8^+$ T cells derived from healthy HLA-$A24^+$ donors with latent EBV infection. We used an HLA-A*2402–restricted major histocompatibility complex (MHC) tetramer mixture of five EBV epitopes (BRLF-1, BMLF-1, latent membrane protein 2 (LMP2), Epstein-Barr nuclear antigen 3A (EBNA3A) and EBNA3B)[7] to detect EBV-specific $CD8^+$ T cells. We detected varying frequencies (0.00–0.64%) of tetramer-positive cells within the $CD8^+$ T cell populations from 19 HLA-$A24^+$ donors (**Fig. 2a** and **Supplementary Table 1**). We then used FACS to sort single tetramer-positive cells from ten donors whose frequencies of tetramer-positive cells were more than 0.06% of $CD8^+$ T cells (with donor I having the minimum frequency of 0.06%). The efficacy of amplifying the TCRα and TCRβ cDNA pairs from the sorted single T cells was 13–72%, using the 5′ rapid amplification of cDNA ends (RACE) method[5] (**Supplementary Table 2**).

We then analyzed the obtained TCR pairs from each donor. A small population expressed dual TCRα, dual TCRβ or both. In some donors, a large number of T cells expressed dual TCRα or dual TCRβ. This may be due to clonal expansion (**Supplementary Table 3**). In total, we obtained 380 EBV-specific TCRs from ten healthy donors with latent EBV infection (**Supplementary Table 2**).

The diversity of the EBV-specific TCRs was highly restricted (from one to ten in each donor) (**Fig. 2b** and **Supplementary Fig. 2**). Because

[1]Department of Immunology, Graduate School of Medicine and Pharmaceutical Sciences, University of Toyama, Toyama, Japan. [2]Department of Gastroenterology, Graduate School of Medicine, Kanazawa University, Kanazawa, Ishikawa, Japan. [3]College of Basic Medical Science, Harbin Medical University, Harbin, China. [4]These authors contributed equally to this work. Correspondence should be addressed to H.K. (immkishi@med.u-toyama.ac.jp).

Received 2 April 2012; accepted 8 April 2013; published online 13 October 2013; doi:10.1038/nm.3358

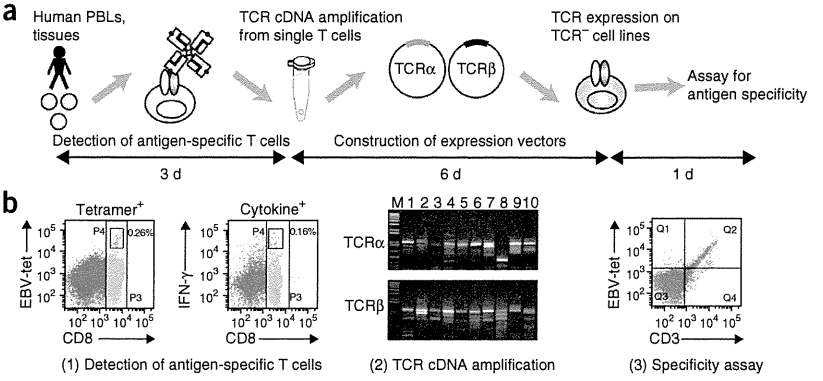

Figure 1 Schematic of the hTEC10 system. (**a**) A schematic depicting the procedure of the hTEC10 system. Briefly, human TCR cDNAs were amplified from single cells, cloned into an expression vector and then transduced into the TCR-negative T cell line TG40. The antigen specificity of TCRs was then assessed by staining the TG40 cells with MHC tetramers or by monitoring CD69 expression. The entire process can be performed within 10 d. (**b**) Detection of antigen-specific T cells with MHC tetramers (left) or cytokine secretion (right) (1), analysis of amplified TCRαβ chain cDNA (2) and examination of TCR expressed on TG40 cells using EBV tetramer (EBV-tet) binding (3).

the TCR repertoire of the tetramer-negative cells was not skewed toward a particular TCRα V or TCRβ V subgroup (**Supplementary Fig. 3**), the skewing of the TCR repertoire in the tetramer-positive cells was not due to PCR bias. Notably, our system can clone rare antigen-specific T cell clones (indicated by asterisks in **Fig. 2b** and **Supplementary Fig. 2**) that may be missed when using conventional cloning methods.

To determine the antigen specificity of the cloned TCRs, we first transferred the cDNA into TG40 cells and stained the cells with MHC-peptide tetramer mixture. The tetramer mixture bound to 95% of the cloned TCRs that were expressed on the TG40 cells (**Fig. 2c**). We then determined the antigenic peptide specificity of the cloned TCRs by stimulating the TCR-expressing TG40 cells with HLA-A24⁺ PBLs that were pulsed with each of the EBV peptides (BRLF-1, BMLF-1, LMP2, EBNA3A or EBNA3B), followed by examining the cell-surface expression of CD69 with flow cytometry. The percentages of TCRs specific for BRLF-1, BMLF-1, EBNA3A, EBNA3B and LMP-2 among the EBV-specific TCRs were 65.5%, 12.6%, 19.7%, 1.6% and 0.5%, respectively (**Fig. 2d** and **Supplementary Table 4**).

EBV-specific TCR cDNA–transduced T cells kill target cells

To determine the cytotoxic activity of EBV-specific TCR cDNA–transduced T cells, we transduced cDNAs encoding BRLF-1–specific

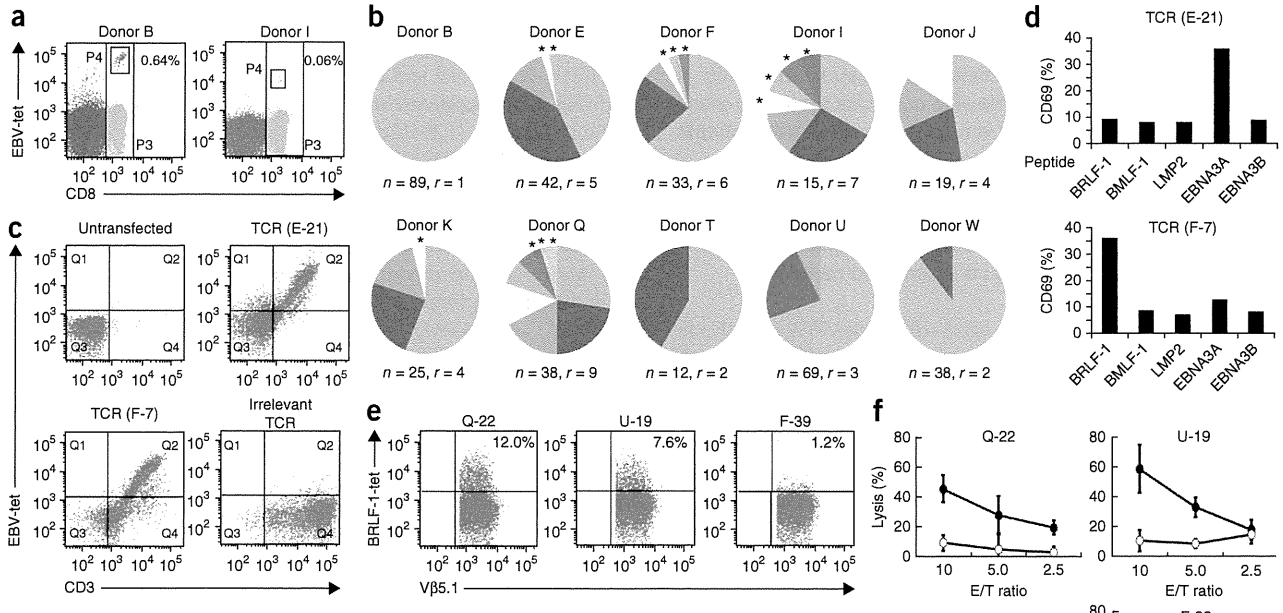

Figure 2 Analysis of EBV-specific human TCRαβ pairs obtained by hTEC10. (**a**) Flow cytometric analysis of EBV-specific CD8⁺ T cells in human PBLs by staining with CD8-specific antibody and HLA-A*2402 EBV tetramers. Data for two out of ten donors are shown (donors B and I). The experiments were performed only once for each donor. (**b**) TCR repertoire analysis of EBV-specific CD8⁺ T cells from ten latent healthy donors. *n*, number of analyzed T cell clones; *r*, repertoire number; asterisks, repertoire obtained from only a single T cell clone. (**c**) Determination of TCR antigen specificity by staining of TCR cDNA–transduced TG40 cells with CD3-specfic antibody and EBV tetramer mixture. Data for two TCRs out of analyzed EBV-specific TCRs are shown (E-21 and F-7 TCR). The experiments were performed twice for each TCR. (**d**) Flow cytometric analysis of CD69 expression in TG40 cells expressing E-21 or F-7 TCRs in the presence of various EBV-derived peptides and HLA-A24⁺ PBLs. (**e**) TCR expression analysis of BRLF-1–specific Vβ5.1⁺ TCRs (Q-22, U-19 or F-39) on TCR cDNA–transduced primary T cells by staining with Vβ5.1-specific antibody and BRLF-1–specific tetramer (BRLF-1-tet). Profile of only Vβ5.1⁺ population is shown. The percentage of Vβ5.1 was 15.4%, 19.1% and 16.9% of PBLs for Q-22, U-19 and F-39, respectively. The percentage of tetramer-positive cells in Vβ5.1⁺ cell population is indicated. Representative data of three independent experiments are shown. (**f**) Cytotoxicity of TCR cDNA–transduced primary T cells against T2-A24 cells pulsed with BRLF-1 peptide (closed circle) or EBNA3A peptide (open circle) labeled with calcein. The results shown are mean ± s.d. of triplicate experiments. E/T ratio, ratio of effector T cells to target cells.

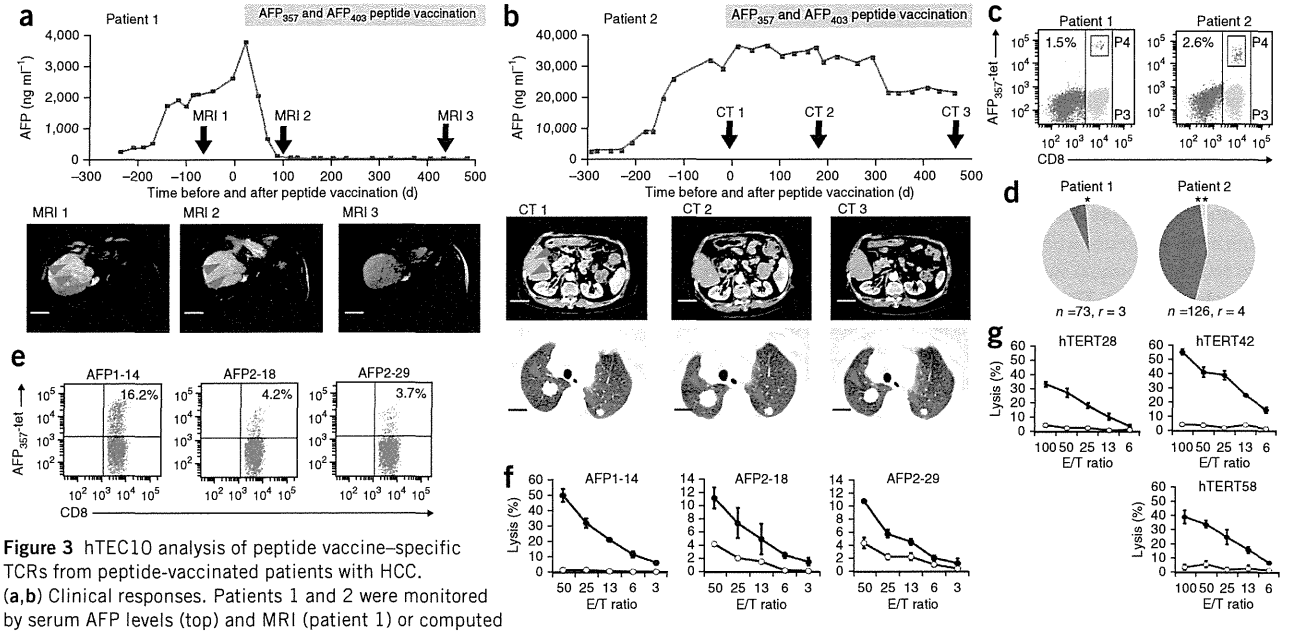

Figure 3 hTEC10 analysis of peptide vaccine–specific TCRs from peptide-vaccinated patients with HCC. (**a**,**b**) Clinical responses. Patients 1 and 2 were monitored by serum AFP levels (top) and MRI (patient 1) or computed tomography (patient 2) (bottom). Black arrows show examination dates and red arrowheads show metastatic lesions of HCC. Scale bars in **a**, 50 mm; in **b**, 50 mm (top) and 30 mm (bottom). (**c**) Detection of AFP_{357} peptide–specific $CD8^+$ T cells of PBLs in patients with HCC with CD8-specific antibody and AFP_{357}-specific tetramers. Percentages of AFP_{357}-specific tetramer-positive cells in $CD8^+$ T cells are indicated. (**d**) Repertoire of AFP_{357} $tetramer^+$ $CD8^+$ T cells. *n*, number of analyzed T cell clones; *r*, repertoire number; asterisk, repertoire obtained from only a single T cell clone. (**e**) Expression of AFP_{357}-specific TCRs on TCR cDNA–transduced primary T cells. Profile of only $CD8^+$ population is shown. Percentages of AFP_{357}-specific tetramer-positive cells among $CD8^+$ T cells are indicated. (**f**) Cytotoxicity of AFP-specific TCR cDNA–transduced primary T cells toward C1R-A24 cells pulsed with AFP_{357}-peptide (closed circle) or control peptide (open circle). Data are expressed as mean ± s.d. of triplicate experiments. Representative data of three independent experiments are shown. (**g**) Cytotoxicity of hTERT–specific TCR cDNA–transduced primary T cells toward C1R-A24 cells pulsed with $hTERT_{461}$ peptide (closed circle) or control peptide (open circle). Data are expressed as mean ± s.d. of triplicate experiments. Representative data of three independent experiments are shown.

Vβ5.1$^+$ TCRs (clones Q-22, U-19 and F-39) into primary human T cells using retroviral vectors and compared their ability to kill T2-A24 cells, a TAP-deficient T2 cell line expressing HLA-A*2402 (ref. 8), that had been pulsed with the BRLF-1 peptide. These three TCRs have the same Vβ region (Vβ5.1$^+$) but distinct CDR3 sequences and Vα regions. The BRLF-1 tetramer bound to 12.0%, 7.6% and 1.2% of Vβ5.1$^+$ cells in the T cell populations that were transduced with Q-22, U-19 and F-39 TCR cDNAs, respectively, whereas the percentages of Vβ5.1$^+$ cells in the Q-22, U-19 and F-39 TCR cDNA transfectants were the same level (**Fig. 2e** and **Supplementary Fig. 4a**). This result indicates that the transduced TCRs tend to mispair with endogenous TCRs[9].

We then determined the cytotoxic activity of T cells that were transduced with the BRLF-1–specific TCR cDNAs against T2-A24 cells that had been pulsed with the BRLF-1 or the EBNA3A peptide. T cells transduced with BRLF-1–specific TCR cDNAs exhibited cytotoxicity toward the BRLF-1 peptide–pulsed T2-A24 cells but not toward the EBNA3A peptide–pulsed cells (**Fig. 2f**), demonstrating that the cytotoxic activity was peptide specific. Similarly, T cells transduced with EBNA3A-specific TCR (E-21) cDNAs demonstrated cytotoxicity toward EBNA3A peptide–pulsed T2-A24 cells but not BRLF-1 peptide–pulsed cells (**Supplementary Fig. 5a**,**c**).

We also measured the cytokine secretion of the TCR cDNA–transduced T cells after antigen stimulation. Peripheral blood lymphocytes (PBLs) transduced with BRLF-1–specific TCR cDNAs (Q-22, U-19 and F-39) secreted multiple cytokines (interferon-γ (IFN-γ), tumor necrosis factor-α (TNF-α) and interleukin-2 (IL-2)) upon stimulation with the BRLF-1 peptide, but not with the EBNA3A peptide (**Supplementary Fig. 6**). In contrast, PBLs transduced with the EBNA3A-specific TCR (E-21) cDNAs secreted IFN-γ upon stimulation with the EBNA3A peptide but with the BRLF-1 peptide (**Supplementary Fig. 5b**).

Furthermore, we examined the functional avidity of the EBV-specific TCRs using the TG40-based TCR downregulation assay, and we determined the half-maximum inhibitory concentration (IC_{50}) of the peptide responses. The Q-22 TCR exhibited the highest functional avidity (**Supplementary Fig. 7** and **Supplementary Table 5**). Therefore, we examined whether T cells transduced with the Q-22 TCR cDNA could respond to EBV-transformed lymphoblastoid cell line (LCL) cells endogenously expressing the EBV antigen and HLA-A*2402 (JTK-LCL cells). The Q-22 TCR cDNA–transduced T cells exhibited a marked response to JTK-LCL cells and produced IFN-γ (**Supplementary Fig. 8**). However, we did not detect CTL activity of the Q-22 TCR cDNA–transduced T cells against JTK-LCL cells. These data are in agreement with a previous report[7]. This lack of cytotoxicity may be owing to limited presentation of the BRLF-1 peptide by HLA-A*2402 on the cell surface of JTK-LCL cells.

In summary, we obtained 380 EBV-specific TCRαβ cDNA pairs and analyzed the TCR repertoires. All of the cloned TCRs were previously uncharacterized (**Supplementary Table 6**).

Clinical application of hTEC10 system in people with cancer

To apply the hTEC10 system to patients with cancer, we obtained PBLs from two patients with hepatocellular carcinoma (HCC) who had been treated with α-fetoprotein (AFP)-derived peptide vaccines and exhibited clinical responses. We show the clinical courses of cancer in these patients (**Fig. 3a**,**b**). The first patient (patient 1), who was infected with hepatitis B virus (HBV) and had a large HCC tumor with vascular invasion of

the portal vein, was vaccinated with the AFP_{357} and AFP_{403} peptides biweekly for 72 weeks. After vaccination, the patient's elevated serum AFP value was normalized; the size of the HCC tumor also decreased, and it eventually disappeared, as evaluated by magnetic resonance imaging (MRI) (**Fig. 3a**), indicating a complete response. The second patient (patient 2), who was infected with HBV and had multiple metastatic HCC lesions in the abdominal wall and lungs, was vaccinated with the AFP_{357} and AFP_{403} peptides biweekly for 88 weeks. After vaccination, the patient's elevated serum AFP value decreased, and the metastatic HCC lesions in the abdominal wall disappeared, as evaluated by computed tomography (**Fig. 3b**). The size and number of lung metastases did not change over the 88 weeks of treatment, indicating stable disease.

We examined whether AFP_{357}-specific T cells could be detected in the PBLs of patients 1 and 2 before or during vaccination by employing an AFP_{357}-specific tetramer and flow cytometry. We could not detect AFP-specific $CD8^+$ T cells detected in the PBLs of the patients either before or during treatment (**Supplementary Fig. 9**). However, when we incubated the PBLs with AFP-derived peptides for 3 weeks to expand the AFP-specific $CD8^+$ T cells, we detected AFP_{357}-specific T cells in the PBLs obtained from both patients during vaccination but not from the PBLs obtained before vaccination (**Supplementary Fig. 10**). These data indicate that the detection of AFP_{357}-specific TCRs in the patients' PBLs was due to peptide vaccination.

1.5% and 2.6% of the $CD8^+$ T cells were positive for tetramer staining in patients 1 and 2, respectively (**Fig. 3c**). We then sorted the single AFP tetramer–positive $CD8^+$ T cells, amplified the TCR cDNAs and analyzed their sequences. We obtained 73 and 126 AFP-specific TCRs from patients 1 and 2, respectively. The sequence analysis revealed that the hTEC10 system yielded three and four T cell clones from patients 1 and 2, respectively (**Fig. 3d**), suggesting that peptide vaccination induced the oligoclonal expansion of AFP-specific T cells in these patients. Alternatively, *in vitro* culture may have resulted in the oligoclonal expansion of AFP-specific T cells. In contrast to EBV-specific TCRs, the repertoires of AFP-specific TCRs might be biased by *in vitro* culture, as suggested by Zhou *et al.*[10]. Notably, the hTEC10 system could clone TCRs from very rare antigen-specific T cells, as in the case of EBV-specific minor clones (**Fig. 3d**).

We then transduced three of the obtained AFP-specific TCR cDNAs into primary T cells of a healthy donor and analyzed the binding of the AFP tetramer. The TCR cDNAs were transduced into 28–32% of the T cells (**Supplementary Fig. 4b**), and 3.7–16.2% of the total $CD8^+$ cells bound the AFP tetramer (**Fig. 3e**). We then determined the cytotoxic activity of the transduced T cells toward C1R-A24 cells (an LCL transfected with HLA-A*2402)[11] pulsed with the AFP peptide. The T cells transduced with these TCR cDNAs showed marked cytotoxicity toward AFP peptide–pulsed C1R-A24 cells but not control peptide ($HIV_{584-592}$)-pulsed cells (**Fig. 3f**), indicating that the cytotoxic activity was peptide specific. We also measured cytokine secretion by the TCR cDNA–transduced T cells after antigen stimulation. PBLs transduced with AFP_{357}-specific TCR cDNAs (AFP1-14, AFP2-28 and AFP2-29), but not PBLs transduced with control GFP vector, secreted IFN-γ when stimulated with the AFP_{357} peptide (**Supplementary Fig. 11**).

Next, we examined the cytotoxic activity of the T cells transduced with AFP-specific TCR cDNAs to HepG2 cells, which endogenously express AFP[11]. However, they did not show any specific cytotoxicity to the target cells (data not shown). We also obtained four kinds of human telomerase reverse transcriptase (hTERT)-specific TCRs from patients with HCC who had been vaccinated with hTERT peptide in the clinical trial (**Supplementary Fig. 12**). We transduced three hTERT-specific TCR cDNAs in primary T cells and examined their cytotoxic activity toward hTERT peptide–pulsed C1R-A24 cells or HepG2 cells that endogenously expressed hTERT. The T cells transduced with human TERT-specific TCR cDNAs (hTERT28, hTERT42 and hTERT58) showed marked cytotoxicity toward hTERT peptide–pulsed C1R-A24 cells (**Fig. 3g**). However, they did not show marked cytotoxicity toward HepG2 cells (data not shown). These results demonstrate that the hTEC10 system can clone functional TAA peptide–specific TCRs from patients with cancer.

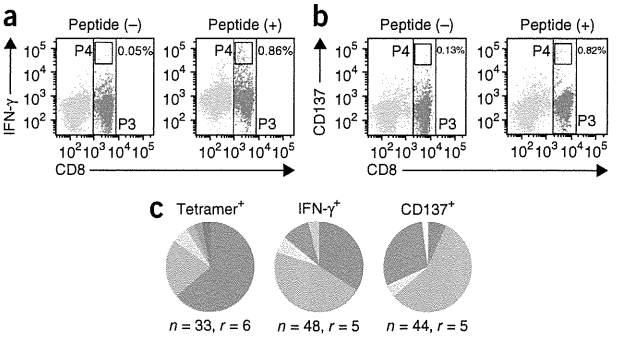

Figure 4 Repertoire analysis of cytokine-secreting $CD8^+$ T cells by stimulation with a specific peptide. (**a**) Secretion of IFN-γ by BRLF-1 peptide–stimulated PBLs. Percentages of IFN-γ–secreting cells in $CD8^+$ T cells are indicated. (**b**) Upregulation of CD137 on BRLF-1 peptide–stimulated PBLs. (**c**) Repertoires of IFN-γ^+ $CD8^+$ T cells and $CD137^+$ $CD8^+$ T cells. *n*, number of analyzed T cell clones; *r*, repertoire number. The same color denotes the same Vα or Vβ repertoires.

Improvement of the hTEC10 system

We next established new MHC tetramer-independent systems to clone TCR cDNAs using cytokine secretion and CD137 upregulation. We obtained PBLs from healthy donors with latent EBV infection and incubated these cells with the BRLF-1 peptide to expand the BRLF-1–specific $CD8^+$ T cells *in vitro*. We then stimulated the expanded BRLF-1–specific $CD8^+$ T cells in the presence of CD28-specific antibody with or without the BRLF-1 peptide and examined IFN-γ secretion or CD137 upregulation. 0.86% of the $CD8^+$ T cells were IFN-γ positive, and 0.82% of the $CD8^+$ T cells had upregulated CD137 (**Fig. 4a,b**). We then sorted the single T cells and analyzed their TCR sequences. We obtained 48 TCRs from the IFN-γ–secreting cells and 44 TCRs from the CD137-upregulated cells, and we compared the repertoires of these populations with those obtained from the MHC-peptide tetramer staining method (**Fig. 4c**).

We found that 86% of the TCR repertoire of the IFN-γ–positive T cells and 68% of that for the CD137-upregulated T-cells was identical to that identified by staining with the MHC-peptide tetramer. We also tested the tetramer-binding ability of five TCR clones that were isolated with the IFN-γ–based protocol and five TCR clones that were isolated with the CD137 upregulation protocol. All of the clones bound the tetramer (data not shown). In addition, we examined the ability of six TCRs that bound the MHC-peptide tetramer (**Supplementary Fig. 13**) to induce IFN-γ production when transduced into PBLs. All six TCR cDNA–transduced PBLs produced IFN-γ (**Supplementary Fig. 14**). Taken together, these results demonstrate that the hTEC10 system can rapidly and efficiently clone TCR cDNAs by assessing cytokine secretion or CD137 upregulation.

DISCUSSION

In this study, we established a system for the rapid and direct cloning and functional evaluation of TCR cDNAs derived from single antigen-specific

human T cells (hTEC10 system). We used this system to obtain and analyze antigen-specific TCRs from healthy donors and patients with cancer.

With regard to minimal frequencies of specific T cells required for the proper identification of TCRs, the frequency of the EBV tetramer$^+$ cells of donor I was the minimum (0.06% of the CD8$^+$ T cells or 0.01% of the total PBLs). We sorted 48 EBV tetramer$^+$ cells from 8×10^6 cells. Twenty-three pairs of TCR α and β cDNAs were amplified. Fifteen of them could be expressed in TG40 cells and could bind EBV tetramer.

Regarding the processing time, the hTEC10 system can obtain antigen-specific TCR cDNAs within 10 d when the antigen-specific T cells are detected on day 1. If the antigen-specific T cells cannot be detected in primary T cells, they need to be cultured for a certain duration. Thus, 8 d, plus additional days for *in vitro* culture, are required to obtain antigen-specific TCRs.

Concerning the EBV-specific TCR repertoires, all of the cloned TCRs were previously uncharacterized. The repertoire of EBV-specific TCRs was highly restricted, in agreement with previous reports[12,13]. The analysis was reproducible, as we obtained similar results from donor B and donor E in two independent experiments.

To determine candidate TCRs for gene therapy for cancer, we used the hTEC10 system to analyze PBLs derived from patients with HCC who had been successfully treated by AFP-derived peptide vaccination. The appropriateness of oncofetal antigens as targets for TCR gene therapy has recently been questioned[14]. However, Butterfield *et al.*[15] previously reported that a phase 1/2 clinical trial of immunization with dendritic cells pulsed with HLA-A*0201–restricted AFP peptides in patients with HCC showed no adverse events. Furthermore, we previously compared the *in vitro* effect of various TAA peptides on PBLs from patients with HCC and showed that HLA-A*2402–restricted AFP peptides may be candidates for peptide vaccination of patients with HCC[11,16]. Thus, a clinical trial to determine the effectiveness of AFP-derived peptide vaccination for patients with HCC has already been conducted, and several patients have exhibited positive clinical responses.

Our data showed that primary T cells transduced with AFP-specific and hTERT-specific TCR cDNAs showed potent antigen-specific cytotoxicity toward AFP- or hTERTpeptide–pulsed target cells, but they did not show marked cytotoxicity toward HepG2 cells that had been reported to endogenously express AFP and hTERT (data not shown). We reasoned three possibilities. The first is that the efficiencies of TCR transduction into PBLs were low. The second is that HepG2 cells may present an insufficient amount of hTERT peptide on their HLA-A24 molecules. The third is the weak affinity of the obtained TCRs. We need to clone more AFP- and hTERT-specific TCRs to acquire TCRs with sufficient affinity to induce cytotoxicity toward HepG2 cells.

Finally, we applied the hTEC10 system to detect and retrieve TCRαβ pair cDNAs by analyzing cytokine secretion and CD137 upregulation. Most of the TCR repertoire of IFN-γ–positive T cells or CD137-upregulated T cells was identical to that identified by the MHC-peptide tetramer, whereas the rest were not identical. These results, along with the CD69 induction assay, indicate that the hTEC10 system can be used with cytokine-secreting or CD137-upregulated CD8$^+$ T cells without the need for staining with an MHC-peptide multimer. Therefore, we can apply the hTEC10 system to isolate T cells from patients with cancer for whom the identity of the tumor antigen is unknown. The T cells can be stimulated with tumor cells, and the IFN-γ–secreting or CD137-upregulated CD8$^+$ cells can be sorted. After cloning the TCRs, their specificity can be examined by analyzing the response of TCR cDNA–transduced T cells to the tumor cells.

METHODS

Methods and any associated references are available in the online version of the paper.

Accession codes. cDNA sequences were deposited in DNA Data Bank of Japan with accession codes from AB749820 to AB749925.

Note: Any Supplementary Information and Source Data files are available in the online version of the paper.

ACKNOWLEDGMENTS

We thank S. Hirota, A. Takishita, K. Shitaoka and M. Horii for technical assistance and K. Hata for secretarial work. This research was supported by grants from the Hokuriku Innovation Cluster for Health Science and a Grant-in-Aid from the Ministry of Education, Culture, Sports, Science and Technology in Japan (11F01415 and 24650630). Retroviral pMX vector, pMX-IRES-EGFP vector and PLAT-E cell line were kindly provided by T. Kitamura (University of Tokyo), human CD8–expressing TG40 cell line by T. Ueno and C. Motozono (Kumamoto University) with permission from T. Saito (Riken), T2-A24 cell line by K. Kuzushima (Aichi Cancer Center Research Institute), Phoenix-A cell line by G. Nolan (Stanford University) and C1R-A24 cell line from M. Takiguchi (Kumamoto University).

AUTHOR CONTRIBUTIONS

E.K., E.M., H.H., T.N. and A.J. performed and analyzed the experiments. E.K., E.M., H.K., S.K., H.N. and A.M. designed the experiments. E.M. and T.O. contributed reagents. E.K., H.K. and A.M. wrote the manuscript, and E.K., E.M., H.K., S.K. and A.M. edited the manuscript.

COMPETING FINANCIAL INTERESTS

The authors declare no competing financial interests.

1. Morgan, R.A. *et al.* Cancer regression in patients after transfer of genetically engineered lymphocytes. *Science* **314**, 126–129 (2006).
2. Johnson, L.A. *et al.* Gene therapy with human and mouse T-cell receptors mediates cancer regression and targets normal tissues expressing cognate antigen. *Blood* **114**, 535–546 (2009).
3. Linnemann, C., Schumacher, T.N. & Bendle, G.M. T-cell receptor gene therapy: critical parameters for clinical success. *J. Invest. Dermatol.* **131**, 1806–1816 (2011).
4. Uttenthal, B.J., Chua, I., Morris, E.C. & Stauss, H.J. Challenges in T cell receptor gene therapy. *J. Gene Med.* **14**, 386–399 (2012).
5. Ozawa, T., Tajiri, K., Kishi, H. & Muraguchi, A. Comprehensive analysis of the functional TCR repertoire at the single-cell level. *Biochem. Biophys. Res. Commun.* **367**, 820–825 (2008).
6. Dash, P. *et al.* Paired analysis of TCRα and TCRβ chains at the single-cell level in mice. *J. Clin. Invest.* **121**, 288–295 (2011).
7. Kuzushima, K. *et al.* Tetramer-assisted identification and characterization of epitopes recognized by HLA A*2402-restricted Epstein-Barr virus-specific CD8$^+$ T cells. *Blood* **101**, 1460–1468 (2003).
8. Miyahara, Y. *et al.* Determination of cellularly processed HLA-A2402–restricted novel CTL epitopes derived from two cancer germ line genes, MAGE-A4 and SAGE. *Clin. Cancer Res.* **11**, 5581–5589 (2005).
9. Okamoto, S. *et al.* Improved expression and reactivity of transduced tumor-specific TCRs in human lymphocytes by specific silencing of endogenous TCR. *Cancer Res.* **69**, 9003–9011 (2009).
10. Zhou, J., Dudley, M.E., Rosenberg, S.A. & Robbins, P.F. Selective growth, *in vitro* and *in vivo*, of individual T cell clones from tumor-infiltrating lymphocytes obtained from patients with melanoma. *J. Immunol.* **173**, 7622–7629 (2004).
11. Mizukoshi, E., Nakamoto, Y., Tsuji, H., Yamashita, T. & Kaneko, S. Identification of α-fetoprotein–derived peptides recognized by cytotoxic T lymphocytes in HLA-A24$^+$ patients with hepatocellular carcinoma. *Int. J. Cancer* **118**, 1194–1204 (2006).
12. Lim, A. *et al.* Frequent contribution of T cell clonotypes with public TCR features to the chronic response against a dominant EBV-derived epitope: application to direct detection of their molecular imprint on the human peripheral T cell repertoire. *J. Immunol.* **165**, 2001–2011 (2000).
13. Argaet, V.P. *et al.* Dominant selection of an invariant T cell antigen receptor in response to persistent infection by Epstein-Barr virus. *J. Exp. Med.* **180**, 2335–2340 (1994).
14. Parkhurst, M.R. *et al.* T cells targeting carcinoembryonic antigen can mediate regression of metastatic colorectal cancer but induce severe transient colitis. *Mol. Ther.* **19**, 620–626 (2011).
15. Butterfield, L.H. *et al.* A phase I/II trial testing immunization of hepatocellular carcinoma patients with dendritic cells pulsed with four α-fetoprotein peptides. *Clin. Cancer Res.* **12**, 2817–2825 (2006).
16. Mizukoshi, E. *et al.* Comparative analysis of various tumor-associated antigen-specific T-cell responses in patients with hepatocellular carcinoma. *Hepatology* **53**, 1206–1216 (2011).

ONLINE METHODS

Healthy donors and human leukocyte antigen typing. Human experiments were performed with the approval of the Ethical Committee at the University of Toyama, Toyama, Japan. Informed consent was obtained from all subjects. PBLs were isolated as described previously[16]. HLA-A24 and HLA-A02 haplotype positivity was screened by staining PBLs with FITC-conjugated HLA-A24 (clone 17A10) and HLA-A2 (clone BB7.2) antibody (MBL) and analyzed with flow cytometry.

Peptide vaccination of patients. The clinical trial of the HLA-A24–restricted AFP_{357} (EYSRRHPQL) and AFP_{403} (KYIQESQAL) peptide vaccines (trial registration: UMIN000003514) and that of the HLA-A24–restricted $hTERT_{461}$ (VYGFVRACL) peptide vaccines (trial registration: UMIN000003511) were conducted at Kanazawa University Hospital, Kanazawa, Japan. Patients with verified radiological diagnoses of HCC stage III or IV were enrolled in this study. The patients each received 3.0 mg of AFP-derived peptide vaccine in each dose. The peptides, which were synthesized as GMP-grade products at Neo MPS, were administered as an emulsified solution containing incomplete Freund's adjuvant (Montanide ISA-51 VG; SEPPIC) by biweekly subcutaneous immunization for 72 weeks (patient 1) and 88 weeks (patient 2). Clinical responses were monitored by measuring the serum AFP value and carrying out dynamic computed tomography or MRI and were evaluated according to the Response Evaluation Criteria in Solid Tumors, version 1.1. All patients provided written informed consent to participate in the study in accordance with the Helsinki Declaration, and this study was approved by the regional ethics committee (Medical Ethics Committee of Kanazawa University, No. 858). Blood samples from the patients were tested for the surface antigen of the HBV and hepatitis C virus using commercial immunoassays (Fuji Rebio). HLA-based typing of patient PBLs was performed using the polymerase chain reaction–reverse sequence-specific oligonucleotide (PCR-RSSO) method. The serum AFP level was measured by ELISA (Abbott Japan). PBLs were isolated from patients as described previously[16], resuspended in RPMI 1640 medium containing 80% FCS and 10% dimethyl sulfoxide and cryopreserved until use.

Cell culture and cell lines. RPMI 1640 and DMEM media (Wako Pure Chemical) were supplemented with 10% FBS (Biowest), 100 μg ml^{-1} streptomycin and 100 U ml^{-1} penicillin. Human CD8–expressing TG40 cells[17], T2-A24 cells[8] from a transporter associated with antigen presentation (TAP)-deficient T2 cell line transfected with HLA-A*2402 and C1R-A24 cells from a C1R lymphoblastoid cell line transfected with HLA-A*2402 (ref. 11) were maintained in RPMI 1640 medium. PLAT-E[18] and Phoenix-A[19] (a retroviral packaging cell line) and HepG2, (hepatocellular carcinoma cell line, purchased from ATCC), were maintained in DMEM medium.

Antibody and MHC tetramer staining. FITC-conjugated CD8-specific antibody (1: 200, clone T8) and PC5-conjugated CD8-specific antibody (1: 1,000, clone B9.11) were purchased from Beckman Coulter. Phycoerythrin-conjugated CD137-specific antibody (1:40, clone 4B4-1) was purchased from BioLegend. Biotin-conjugated CD3ε-specific antibody (1:200, clone 145-2C11), allophycocyanin-conjugated streptavidin and phycoerythrin-conjugated CD69-specific antibody (1:200, clone H1.2F3) were purchased from eBioscience. EBV-specific T cells were stained with phycoerythrin-conjugated HLA-A*2402–peptide tetramers or HLA-A*0201–peptide tetramers. The sequences of the HLA-A*2402-restricted EBV peptides are as follows: TYPVLEEMF ($BRLF\text{-}1_{198-206}$), DYNFVKQLF ($BMLF\text{-}1_{320-328}$), IYVLVMLVL ($LMP2_{222-230}$), RYSIFFDYM ($EBNA3A_{246-254}$) and TYSAGIVQI ($EBNA3B_{217-225}$). The sequences of the HLA-A*0201-restricted EBV peptides are GLCTLVAML ($BMLF\text{-}1_{280-288}$) and YLQQNWWTL ($LMP1_{159-167}$). AFP-specific or hTERT-specific T cells were stained with the phycoerythrin-conjugated HLA-A*2402 peptide ($AFP_{357-365}$)[11] or HLA-A*2402 peptide ($hTERT_{461-469}$)[20]. All tetramers were purchased from MBL.

Single-cell sorting and RT-PCR. Tetramer-positive cells that had been stimulated with IL-2 and phytohemagglutin for 2 d were single-cell–sorted by FACSAria (Becton Dickinson) into MicroAmp reaction tubes (Applied Biosystems) that contained a cell lysis solution composed of 29.2 μg Dynabeads $Oligo(dT)_{25}$ (Invitrogen), 2.9 μl Lysis/Binding Buffer (Invitrogen) and 0.29 pmol of each gene-specific primer. The sequences of the primers were as follows: alpha-RT 5′-AGCAGTGTTTGGCAGCT CTT-3′, beta1-RT 5′-CTGGCAAAAGAAGAATGTGT-3′ and beta2-RT (5′-ACACAGATTGGGAGCAGGTA-3′). The Dynabeads were then transferred into a solution containing 4.0 U SuperScriptIII (Invitrogen), 0.3 U Murine RNase inhibitor (New England BioLabs), 0.5 mM each dNTP, 5 mM DTT, 0.2% Triton X-100 and 1× First-Strand Buffer (Invitrogen). The reverse transcription reaction was performed for 40 min at 50 °C. After the reverse transcription reaction, the Dynabeads were transferred into another solution containing 8 U of terminal deoxynucleotidyl transferase (Roche), 0.5 mM dGTP, 0.4 U murine RNase inhibitor, 4 mM $MgCl_2$, 0.2% Triton X-100, 50 μM K_2HPO_4 and 50 μM KH2PO4, pH 7.0, and were incubated for 40 min at 37 °C to add a poly-dG tail to the 3′ end of the cDNA. The Dynabeads were then transferred into a new PCR tube containing the first PCR reaction mixture. The first PCR was performed using PrimeSTAR HS DNA polymerase (TaKaRa) according to the manufacturer's instructions with the AP-1, alpha-1st, beta1-1st and beta2-1st primers. The PCR cycles for AP-1 (5′-ACAGCAGGTCAGTCAAGCAGTAGCAGCAGTTCG ATAACTTCGAATTCTGCAGTCGACGGTACCGCGGGCCCGGGATC CCCCCCCCCCCDN-3′), alpha-1st (5′-AGAGGGAGAAGAGGGGCA AT-3′), beta1-1st (5′-CCATGACGGGTTAGAAGCTC-3′) and beta2-1st (5′-GGATGAAGAATGACCTGGGAT-3′) were as follows: 5 min at 95 °C followed by 30 cycles of 15 s at 95 °C, 5 s at 60 °C and 1 min 30 s at 72 °C.

The resultant PCR mixtures were diluted 100-fold with water, and 2 μl of the diluted PCR mixtures were added to 23 μl of the nested PCR mixture as template DNA. The nested PCR was performed in a reaction mixture similar to that for the first PCR but with the adaptor primer AP-2 (5′-AGCAGTAGCAGCAGTTCGATAA-3′) and a primer specific for the constant region of TCRα (alpha-nest, 5′-GGTGAATAGGCAGACAGACTT-3′) or TCRβ (beta-nest, 5′-GTGGCCAGGCACACCAGTGT-3′). The PCR cycles were as follows: 1 min at 98 °C followed by 35 cycles of 15 s at 98 °C, 5 s at 60 °C and 45 s at 72 °C.

The PCR products were then analyzed with the alpha-nest or beta-nest primer by either direct sequencing or sequencing after subcloning into an expression vector. The TCR repertoire was analyzed with the IMGT/V-Quest tool (http://www.imgt.org/)[21].

Retroviral transfection. The cDNAs encoding the TCRα or TCRβ chain were independently inserted into a pMX vector or pMX-IRES-EGFP vector[22], which was then transfected into PLAT-E cells with FuGENE 6 (Roche). The culture supernatant was collected 72 h after transfection and added to human CD8–TG40 cells together with polybrene (Sigma-Aldrich). EBV-specific tetramer binding was analyzed by flow cytometry. For transduction into human PBLs, the TCRα and TCRβ chains were linked by a viral F2A sequence[23] or a P2A sequence[24], cloned into the pMX-IRES-EGFP vector and transfected into the Phoenix A cells. Transduction efficiency was monitored by the expression of EGFP.

Determination of the antigen specificity of cloned TCRs. The antigen specificity of the cloned TCRαβ pairs was analyzed using the CD69 induction assay, tetramer staining or both. Briefly, TCR-expressing human CD8–TG40 cells were incubated overnight with $HLA\text{-}A24^+$ PBLs in the presence of each of the EBV peptides (BRLF-1, BMLF-1, LMP2, EBNA3A or EBNA3B). After incubation, the cell surface expression of CD69 was analyzed by flow cytometry.

Preparation of PBLs transduced with cloned TCR cDNAs. 5×10^5 PBLs were stimulated *in vitro* with CD3/CD28 Dynabeads (Invitrogen) and 30 IU ml^{-1} recombinant hIL-2 (Peprotech) according to the manufacturer's instructions. On day 2, the stimulated PBLs were washed, and 5×10^5 cells were resuspended in the medium containing 30 IU ml^{-1} recombinant hIL-2. The cells were added to each well in the plates that had been coated with 50 μg ml^{-1} retronectin (TaKaRa) and spin-loaded with TCR-encoding retroviral supernatant by centrifuging for 2 h at 1,900*g* at 32 °C. The cells were spun down at 1,000*g* at 32 °C for 10 min and incubated overnight at 37 °C in 5% CO_2. On day 3, the PBLs were transferred onto newly prepared retroviral-coated plates

as on day 2 and cultured with 30 IU ml^{-1} recombinant hIL-2. On day 10, the TCR cDNA–transduced PBLs were evaluated for expression of the appropriate TCR by tetramer staining and flow cytometry.

Cytotoxic T lymphocyte assay. In the case of the AFP-specific and hTERT-specific TCRs, the cytotoxicity of the TCR cDNA–transduced PBLs was measured by the ^{51}chromium release assay[11]. In the case of the EBV-specific TCR, the cytotoxicity of the TCR cDNA–transduced PBLs was measured using the calcein-AM (Wako Pure Chemical) release assay. Briefly, peptide-loaded T2-A24 target cells were labeled with 25 μM calcein-AM for 30 min at 37 °C. Then, the target cells and TCR cDNA–transduced PBLs (effector cells) were plated in 96-well plates at the indicated effector-to-target (E/T) ratios and incubated for 4 h. After incubation, the fluorescence of calcein in the supernatants was measured using FLUOstar OPTIMA microplate reader (BMG LABTECH). The percentage of cytotoxicity was calculated using the following formula: % lysis = (F experiment − F spontaneous)/(F maximal − F spontaneous) × 100.

IFN-γ secretion assay. IFN-γ–secreting cells were detected using the IFN-γ secretion assay (Miltenyi Biotec) according to the manufacturer's instructions. Briefly, PBLs were stimulated with the BRLF-1 peptide for 14 d. After *in vitro* stimulation, the PBLs were stimulated with CD28-specific antibody with or without the BRLF-1-peptide for 6 h. The PBLs were washed and stained with IFN-γ Catch Reagent (Miltenyi Biotec). The PBLs were then suspended in 1 ml medium and incubated for 45 min to allow cytokine secretion. After washing, the PBLs were stained with phycoerythrin-conjugated IFN-γ Detection Reagent (Miltenyi Biotec) and FITC-conjugated CD8-specific antibody.

ELISA assay. ELISA assays were performed according to the manufacturer's instructions. Briefly, 1×10^5 TCR cDNA–transduced PBLs were cocultured with 1×10^5 T2-A24 cells pulsed with specific peptide. After 16 h incubation, the supernatants were collected, and IFN-γ, IL-2 and TNF-α in the supernatant were measured by ELISA (R&D systems). The results shown are the mean ± s.d. of triplicate experiments.

TG40-based TCR downregulation assay. The IC_{50} of the peptide responses of the TCRαβ cDNA–transduced TG40 was determined with TCR downregulation assay[7]. Briefly, human CD8-TG40 cells expressing TCRs specific for BRLF-1 were incubated overnight with T2-A24 cells in the presence of various concentrations of BRLF-1 peptide. After incubation, the CD3ε expression was analyzed by flow cytometry. The percentage of CD3ε expression was calculated using the following formula: % CD3ε expression = (CD3ε expression in the presence of indicated concentration of specific peptide)/(CD3ε expression in the absence of specific peptide) × 100. The IC_{50} values were calculated by probit analysis[25].

ELISPOT assay. IFN-γ ELISPOT assays were performed as previously reported[26]. 96-well multiscreen filter plates (Millipore) were coated with 5 μg ml^{-1} human IFN-γ–specific antibody (catalog number DY285, R&D Systems) and blocked with culture medium. Then, EBV-transformed JTL-LCL cells with or without HLA-ABC–specific antibody (clone B9.12.1) (Beckman Coulter) were plated with TCR cDNA–transduced PBLs at the indicated cell numbers and incubated for the indicated times. After incubation, 1 μg ml^{-1} biotin-conjugated human IFN-γ–specific antibody (catalog number BAF285, R&D systems) was added, followed by alkaline phosphatase–conjugated streptavidin (Sigma). After washing, a mixture of 3-bromo-4-chloro-3-indolyl-phosphate toluidine and *p*-nitroblue tetrazolium chloride (Sigma) was added to detect the immunospots.

17. Ueno, T., Tomiyama, H., Fujiwara, M., Oka, S. & Takiguchi, M. Functionally impaired HIV-specific CD8 T cells show high affinity TCR-ligand interactions. *J. Immunol.* **173**, 5451–5457 (2004).
18. Morita, S., Kojima, T. & Kitamura, T. Plat-E: an efficient and stable system for transient packaging of retroviruses. *Gene Ther.* **7**, 1063–1066 (2000).
19. Kinsella, T.M. & Nolan, G.P. Episomal vectors rapidly and stably produce high-titer recombinant retrovirus. *Hum. Gene Ther.* **7**, 1405–1413 (1996).
20. Mizukoshi, E. *et al.* Cytotoxic T cell responses to human telomerase reverse transcriptase in patients with hepatocellular carcinoma. *Hepatology* **43**, 1284–1294 (2006).
21. Giudicelli, V., Chaume, D. & Lefranc, M.P. IMGT/V-QUEST, an integrated software program for immunoglobulin and T cell receptor V-J and V-D-J rearrangement analysis. *Nucleic Acids Res.* **32**, W435–W440 (2004).
22. Onishi, M. *et al.* Applications of retrovirus-mediated expression cloning. *Exp. Hematol.* **24**, 324–329 (1996).
23. Ryan, M.D., King, A.M. & Thomas, G.P. Cleavage of foot-and-mouth disease virus polyprotein is mediated by residues located within a 19 amino acid sequence. *J. Gen. Virol.* **72**, 2727–2732 (1991).
24. Leisegang, M. *et al.* Enhanced functionality of T cell receptor-redirected T cells is defined by the transgene cassette. *J. Mol. Med. (Berl)* **86**, 573–583 (2008).
25. Goldstein, A. *Biostatistics: An Introductory Text* (Macmillan, New York, 1964).
26. Jin, A. *et al.* A rapid and efficient single-cell manipulation method for screening antigen-specific antibody-secreting cells from human peripheral blood. *Nat. Med.* **15**, 1088–1092 (2009).

HEPATOLOGY
Official Journal of the American Association for the Study of Liver Diseases

Enhancement of Tumor-Associated Antigen-Specific T Cell Responses by Radiofrequency Ablation of Hepatocellular Carcinoma

Eishiro Mizukoshi, Tatsuya Yamashita, Kuniaki Arai, Hajime Sunagozaka, Teruyuki Ueda, Fumitaka Arihara, Takashi Kagaya, Taro Yamashita, Kazumi Fushimi, and Shuichi Kaneko

Radiofrequency ablation (RFA) is one of the treatments for hepatocellular carcinoma (HCC) and is known to enhance host immune response. However, the epitopes to which enhanced immune responses occur, the impact on patient prognosis, and the functions and phenotype of T cells induced are still unclear. To address these issues, we analyzed immune responses before and after RFA in 69 HCC patients using 11 tumor-associated antigen (TAA)-derived peptides that we identified to be appropriate to analyze HCC-specific immune responses. The immune responses were analyzed using enzyme-linked immunospot (ELISPOT) assay and tetramer assays using peripheral blood mononuclear cells. An increase in the number of TAA-specific T cells detected by interferon-γ ELISPOT assays occurred in 62.3% of patients after RFA. The antigens and their epitope to which enhanced T cell responses occur were diverse, and some of them were newly induced. The number of TAA-specific T cells after RFA was associated with the prevention of HCC recurrence, and it was clarified to be predictive of HCC recurrence after RFA by univariate and multivariate analyses. The number of TAA-specific T cells after RFA was inversely correlated with the frequency of $CD14^{+}HLA\text{-}DR^{-/low}$ myeloid-derived suppressor cells (MDSCs). The modification of T cell phenotype was observed after RFA. The number of TAA-specific T cells at 24 weeks after RFA was decreased. *Conclusion*: Although RFA can enhance various TAA-specific T cell responses and the T cells induced contribute to the HCC recurrence-free survival of patients, besides immunosuppression by MDSCs, the memory phenotype and lifetime of TAA-specific T cells are not sufficient to prevent HCC recurrence completely. Additional treatments by vaccine or immunomodulatory drugs might be useful to improve the immunological effect of RFA. (HEPATOLOGY 2013; 57:1448-1457)

Hepatocellular carcinoma (HCC) is the sixth most frequent type of cancer worldwide, and it is becoming an important public health concern due to its increased incidence in Western and Asian countries.[1,2] Although there are many types of treatments for HCC, the posttreatment recurrence rate is very high.[3] To inhibit HCC recurrence and improve prognosis, an immunotherapeutic approach is considered an attractive strategy.

Radiofrequency ablation (RFA) is one of the treatments for HCC and is now widely used for curative strategies.[4] In recent studies, it has been reported that

Abbreviations: AFP, alpha-fetoprotein; CMV, cytomegalovirus; CT, computed tomography; ELISPOT, enzyme-linked immunospot; HCV, hepatitis C virus; HIV, human immunodeficiency virus; HLA, human leukocyte antigen; IFN-γ, interferon-γ; MDSC, myeloid-derived suppressor cell; MRI, magnetic resonance imaging; PBMC, peripheral blood mononuclear cell; RFA, radiofrequency ablation; TAA, tumor-associated antigen.

From the Department of Gastroenterology, Graduate School of Medicine, Kanazawa University, Kanazawa, Japan.

Received January 4, 2012; accepted October 23, 2012.

Supported in part by grants from the Ministry of Education, Culture, Sports, Science and Technology of Japan.

Address reprint requests to: Shuichi Kaneko, M.D., Department of Gastroenterology, Graduate School of Medicine, Kanazawa University, Kanazawa, Ishikawa 920-8641, Japan. E-mail: skaneko@m-kanazawa.jp; fax: (81)-76-234-4250.

View this article online at wileyonlinelibrary.com.

DOI 10.1002/hep.26153

Potential conflict of interest: Nothing to report.

Additional Supporting Information may be found in the online version of this article.

RFA creates a tumor antigen source for the generation of antitumor immunity and enhances host immune responses.[5] Our previous mouse study also showed that RFA induced antitumor immune responses with massive T cell infiltration into a tumor, and the effect was enhanced by an active variant of CC chemokine ligand 3.[6] These studies suggest that additional immunological approaches to RFA may reduce HCC recurrence after treatment. However, in human studies, important data needed to develop a new immunotherapeutic approach have been lacking. First, the types of tumor-associated antigens (TAAs) and the epitopes to which these enhanced immune responses occur have not been fully identified. Second, the proportion of patients with enhanced antitumor immune responses and the effect of antitumor immunity for a patient's prognosis after RFA are still unclear. Third, the factors that affect TAA-specific immune responses and the functions and phenotype of T cells induced by RFA have not been identified.

In the present study, we analyzed immune responses in peripheral blood mononuclear cells (PBMCs) before and after RFA in 69 HCC patients using 11 TAA-derived peptides that we identified previously to be appropriate for analyzing HCC-specific immune responses. This approach offers useful information to develop a new strategy for HCC immunotherapy and improve the prognosis of patients treated by RFA.

Patients and Methods

Patients and Laboratory Testing. In this study, we examined 69 human leukocyte antigen (HLA)-A24–positive HCC patients with RFA. The diagnosis of HCC was histologically confirmed in 11 patients. For the remaining 58 patients, the diagnosis was based on typical hypervascular tumor staining on angiography in addition to typical findings, which showed hyperattenuated areas in the early phase and hypoattenuation in the late phase on dynamic CT.[7]

RFA was performed with a cool-tip RFA system consisting of an 18-gauge, cooled-tip electrode with a 2- or 3-cm exposed tip (Radionics, Burlington, MA) and radiofrequency generator (CC-1 Cosman Coagulator, Radionics). After local anesthesia, the electrode was inserted through a guide needle under ultrasound guidance. Radiofrequency energy was delivered for 6 to 12 minutes for each session. The energy was increased from 40 watts to 120 watts in a stepwise fashion. During ablation, the electrode was cooled by circulating ice-cooled saline in the electrode lumen to maintain the tip temperature below 20°C. During each treatment, the electrode tip was inserted into the tumor 1-3 times until the target tumor was surrounded by a high-echoic area. Complete necrosis after RFA was confirmed by dynamic computed tomography (CT) or magnetic resonance imaging (MRI). RFA was repeated in some cases until complete necrosis was confirmed. Thirty-nine and 30 patients received RFA 1 and 2-4 times, respectively. After treatments, HCC recurrence was evaluated with dynamic CT or MRI every 3-4 months.

All patients gave written informed consent to participate in the study in accordance with the Helsinki declaration, and this study was approved by the regional ethics committee (Medical Ethics Committee of Kanazawa University).

Blood samples were tested for hepatitis B surface antigen and hepatitis C virus (HCV) antibody using commercial immunoassays (Fuji Rebio, Tokyo, Japan). The patients with HCV antibody were tested for serum HCV RNA by real-time PCR (Roche, Tokyo, Japan), and 49 of 52 patients with HCV antibody were HCV RNA–positive. HLA-based typing of PBMCs from patients and normal blood donors was performed using reverse sequence-specific oligonucleotide analysis with polymerase chain reaction (PCR-RSSO). The serum alpha-fetoprotein (AFP) level was measured via enzyme immunoassay (AxSYM AFP, Abbott Japan, Tokyo, Japan), and the pathological grading of tumor cell differentiation was assessed according to the general rules for the clinical and pathological study of primary liver cancer.[8] The severity of liver disease was evaluated according to the criteria of Desmet et al. using biopsy specimens of liver tissue, where F4 was defined as cirrhosis.[9] Fifty-five patients who participated in the present study received liver biopsy with RFA. Another 14 patients received liver biopsy 1-3 years before RFA.

Peptides and Preparation of PBMCs. Eleven peptides that we previously identified as being useful for analysis of immune response in HLA-A24–positive HCC patients were selected.[10-13] Human immunodeficiency virus (HIV) envelope-derived peptide ($HIVenv_{584}$)[14] and cytomegalovirus (CMV) pp65-derived peptide ($CMVpp65_{328}$)[15] were also selected as control peptides. Peptides were synthesized at Sumitomo Pharmaceuticals (Osaka, Japan). They were identified using mass spectrometry, and their purities were determined to be >90% by analytical high-performance liquid chromatography. PBMCs were isolated before and 2-4 weeks after HCC treatments as described.[11] In the patients who received RFA 2-4 times, PBMCs were obtained 2-4 weeks after the final treatment. In some patients, PBMCs were also obtained 24 weeks after RFA. PBMCs were resuspended

in Roswell Park Memorial Institute 1640 medium containing 80% fetal calf serum and 10% dimethyl sulfoxide and cryopreserved until use.

Interferon-γ ELISPOT Assay. Interferon-γ (IFN-γ) ELISPOT assays were performed as described.[11] Negative controls consisted of an HIV envelope–derived peptide ($HIVenv_{584}$).[14] Positive controls consisted of 10 ng/mL phorbol 12-myristate 13-acetate (PMA, Sigma) or a CMVpp65-derived peptide ($CMVpp65_{328}$).[15] The colored spots were counted with a KS ELISpot Reader (Zeiss, Tokyo, Japan). The number of specific spots was determined by subtracting the number of spots in the absence of an antigen from the number in its presence. Responses to peptides were considered positive if more than 10 specific spots were detected, which is greater than the mean + 3 SD of the baseline response detected in 11 HLA-A24–positive normal blood donors against TAA-derived peptides, and the number of spots in the presence of an antigen was at least twofold that in its absence. The results of an ELISPOT assay with more than 25 spots in the wells without peptides (control wells) were excluded from the analysis.

IFN-γ ELISPOT assays were also performed using PBMC-depleted $CD4^+$ or $CD8^+$ cells to determine what kind of T cell is responsive to the peptides. In the assay using PBMC-depleted $CD4^+$ or $CD8^+$ cells, the number of cells was adjusted to $3 - 10^5$ cells/well after the depletion. Depletion of $CD4^+$ or $CD8^+$ cells was performed using the MACS separation system with CD4 or CD8 MicroBeads (Miltenyi Biotec, Auburn, CA) in accordance with the manufacturer's instructions.

Detection of Myeloid-Derived Suppressor Cells. For the detection of myeloid-derived suppressor cells (MDSCs), PBMCs were isolated from 20 randomly selected patients 2-4 weeks after HCC treatment. To determine the frequency of $CD14^+HLA\text{-}DR^{-/low}$ MDSCs, two-color fluorescence-activated cell sorting analysis was performed using the following antibodies: anti-CD14 and anti–HLA-DR (Becton Dickinson). Flow cytometry was performed using the FACSAria II system (Becton Dickinson). The frequency of $CD14^+HLA\text{-}DR^{-/low}$ MDSCs was calculated as a percentage of $HLA\text{-}DR^{-/low}$ cells in $CD14^+$ cells.

Tetramer Staining and Flow Cytometry. Peptide $MRP3_{765}$-, AFP_{357}-, AFP_{403}-, and $hTERT_{461}$-specific tetramers were purchased from Medical Biological Laboratories Co., Ltd. (Nagoya, Japan). PBMCs were stained with anti–CD8-APCAb (Becton Dickinson, Tokyo, Japan), anti–CCR7-FITCAb (eBioscience, Tokyo, Japan), anti–CD45RA-PerCP-Cy5.5Ab (eBioscience, Tokyo, Japan), and tetramer-PE for 30 minutes at room temperature. Cells were washed, fixed with 0.5% paraformaldehyde/phosphate-buffered saline, and analyzed using the FACSAria II system.

Table 1. Patient Characteristics (n = 69)

Characteristic	Value
Age, years	67.3 ± 9.4 (69.0)
Sex, male/female	51/18
Platelet count, $\times 10^4/\mu L$	15.9 ± 26.5 (10.9)
Platelet count, $>15 \times 10^4/\leq 15 \times 10^4/\mu L$	19/50
ALT, IU/L	46.7 ± 33.8 (38.0)
ALT, >30/≤30 IU/L	44/25
Prothrombin time, %	78.4 ± 14.6 (77.0)
Prothrombin time, >70%/≤70%	50/19
Albumin, g/dL	3.6 ± 0.5 (3.6)
Albumin, >3.5/≤3.5 g/dL	42/27
Total bilirubin, mg/dL	1.1 ± 0.6 (0.9)
Total bilirubin, >2.0/≤2.0 mg/dL	4/65
AFP, ng/mL	134.7 ± 468.3 (11.0)
AFP, >100/≤100 ng/mL	12/57
HCC differentiation, well/moderate/poor/ND	7/3/1/58
Tumor diameter, >2/≤2 cm	28/41
Tumor multiplicity, multiple/solitary	29/40
Vascular invasion, +/−	1/68
TNM factor	
T1/T2-4	40/29
N0/N1	68/1
M0/M1	69/0
TNM stage, I/II/IIIA/IIIB/IIIC/IV	39/29/0/0/1/0
Histology of nontumor liver, liver cirrhosis/chronic hepatitis	55/14
Liver function, Child-Pugh score A/B/C	52/17/0
Etiology, HCV/HBV/other	52/8/9
Additional treatment,* +/−	14/55

Data are expressed as the mean ± SD (median) or as the number of patients.

Abbreviations: ALT, alanine aminotransferase; HBV, hepatitis B virus; ND, not determined, TNM, tumor-node-metastasis.

*Transarterial embolization.

Statistical Analysis. Data are expressed as the mean ± SD. The estimated probability of tumor recurrence-free survival was determined using the Kaplan-Meier method. The Mantel-Cox log-rank test was used to compare curves between groups. The prognostic factors for tumor recurrence-free survival were analyzed for statistical significance using the Kaplan-Meier method (univariate) and the Cox proportional hazard model (multivariate). Linear regression lines for the relationship between the frequency of $CD14^+HLA\text{-}DR^{-/low}$ MDSCs and the number of TAA-specific T cells were calculated using Pearson's correlation coefficient. A level of $P < 0.05$ was considered significant.

Results

Patient Profile. The clinical profiles of the 69 patients analyzed in the present study are shown in Table 1. HCC was histologically classified as well, moderately, and poorly differentiated in 7, 3, and 1 cases,

Table 2. Peptides and Response Frequency

Peptide Name	Amino Acid Sequence	Number of Specific Spots in Normal Donors (mean ± SD)	Frequency of T Cell Response		P*
			Before RFA	After RFA	
$SART2_{899}$	SYTRLFLIL	1.0 ± 1.4	0/69 (0.0%)	14/69 (20.3%)	<0.001
$SART3_{109}$	VYDYNCHVDL	2.1 ± 1.9	7/69 (10.1%)	20/69 (29.0%)	0.009
$MRP3_{503}$	LYAWEPSFL	0.2 ± 0.5	3/69 (4.3%)	17/69 (24.6%)	0.001
$MRP3_{692}$	AYVPQQAWI	1.5 ± 2.1	4/68 (5.9%)	8/69 (11.6%)	0.366
$MRP3_{765}$	VYSDADIFL	0.9 ± 1.0	3/69 (4.3%)	17/69 (24.6%)	0.001
AFP_{357}	EYSRRHPQL	1.8 ± 2.0	3/68 (4.4%)	14/68 (20.6%)	0.008
AFP_{403}	KYIQESQAL	1.1 ± 1.5	9/66 (13.6%)	24/68 (35.3%)	0.005
AFP_{434}	AYTKKAPQL	0.8 ± 1.1	7/68 (10.3%)	14/68 (20.6%)	0.153
$hTERT_{167}$	AYQVCGPPL	0.8 ± 1.1	9/65 (13.8%)	15/68 (22.1%)	0.263
$hTERT_{324}$	VYAETKHFL	0.5 ± 0.7	6/62 (9.7%)	9/68 (13.2%)	0.591
$hTERT_{461}$	VYGFVRACL	0.7 ± 1.2	11/64 (17.2%)	23/69 (33.3%)	0.046
HIV env_{584}	RYLRDQQLL	1.3 ± 2.0	1/63 (1.6%)	2/68 (2.9%)	>0.999
CMV $pp65_{328}$	QYDPVAALF	13.3 ± 15.7	43/68 (63.2%)	39/67 (58.2%)	0.599

*Analysis via chi-squared test.

respectively. In the other cases, HCC was diagnosed on the basis of typical CT findings and elevated AFP levels. In terms of size and number, the tumor was classified as large (>2 cm) in 28 cases, small (≤2 cm) in 41 cases, multiple in 29 cases, and solitary in 40 cases. Vascular invasion was noted in one patient. Using tumor-node-metastasis staging of the Union Internationale Contre Le Cancer (UICC) system (6th edition),[16] patients were classified as having stage I (n = 39), II (n = 29), IIIA (n = 0), IIIB (n = 0), IIIC (n = 1), or IV (n = 0) tumors.

Detection of TAA-Specific T Cells Before and After RFA. Detection of TAA-specific T cells was performed by direct *ex vivo* analysis (IFN-γ ELISPOT assay). Positive T cell responses against each TAA-derived peptide were observed in 0 to 11 (0.0%-17.2%) patients before RFA (Table 2). The same responses against HIV- and CMV-derived peptides were observed in 1 (1.6%) and 43 (62.3%) patients, respectively. After HCC treatments with RFA, positive T cell responses against TAA-, HIV- and CMV-derived peptide were observed in 8-24 (11.6%-35.3%), 2 (2.9%), and 39 (58.2%) patients, respectively. The increase of the frequency of TAA-specific T cells after RFA observed in 7 of 11 peptides ($SART2_{899}$, $SART3_{109}$, $MRP3_{503}$, $MRP3_{765}$, AFP_{357}, AFP_{403}, and $hTERT_{461}$) was statistically significant (Table 2).

The magnitude of TAA-specific T cell responses determined by the frequency of T cells and the proportion of the patients who showed a significant increase of TAA-specific T cells are shown in Fig. 1. When the T cell responses against a single peptide with more than or equal to 10 specific spots and two-fold increase were defined as significant, a significant increase was observed in 4-16 (6.5%-24.6%) patients for each TAA-derived peptide and in 24 (39.3%) patients for total of TAA-derived peptides. On the other hand, the numbers of patients who showed a significant increase against HIV- and CMV-derived peptide were 1 (1.6%) and 8 (11.9%), respectively. The number of patients who showed a significant increase against at least one TAA-derived peptide after RFA was 43 (62.3%).

To determine what kind of T cell is responsive to the peptides, TAA-derived peptide-specific IFN-γ–producing T cells were also analyzed by ELISPOT assay using PBMC-depleted $CD4^+$ or $CD8^+$ cells. The assay showed that IFN-γ–producing T cells against the peptides ($SART2_{899}$, $SART3_{109}$, $MRP3_{503}$, $MRP3_{692}$, $MRP3_{765}$, AFP_{357}, AFP_{403}, AFP_{434}, $hTERT_{167}$, $hTERT_{324}$, and $hTERT_{461}$) mainly consisted of $CD8^+$ cells (Supporting Fig. 1).

Effect of Increase of TAA-Specific T Cells After RFA for the Prognosis of Patients. To examine the effect of increase of TAA-specific T cells after RFA for the prognosis of patients, we analyzed the relationship between the number of TAA-specific T cells and HCC recurrence-free survival after RFA. First, we divided the patients into two groups with high (above median) and low (below median) specific spots detected via ELISPOT assay. In the analysis, we found that a high number of TAA-specific T cells after HCC treatment correlated significantly with the length of HCC recurrence-free survival ($P = 0.044$) (Fig. 2A). The difference between the groups was emphasized when 50 spots were defined as highly specific spots ($P = 0.006$) (Fig. 2B). On the other hand, there was no correlation between the number of TAA-specific T cells before HCC treatment and the length of HCC recurrence-free survival ($P = 0.758$) (Fig. 2C). Furthermore, the magnitude of enhancement of TAA-specific immune responses did not correlate significantly with the length of HCC recurrence-free survival ($P = 0.267$) (Fig. 2D).

Patients	Peptides														
	$SART2_{899}$	$SART3_{109}$	$MRP3_{503}$	$MRP3_{692}$	$MRP3_{765}$	AFP_{357}	AFP_{403}	AFP_{434}	$hTERT_{167}$	$hTERT_{324}$	$hTERT_{461}$	Total of TAA-derived peptides	$HIVenv_{584}$	$CMVpp65_{328}$
1	0/3	0/13	0/9	0/14	0/6	0/0	0/1	7/1	9/12	0/0	2/0	18/59	0/0	34/65
2	0/1	0/2	0/4	0/0	0/2	0/1	1/1	0/1	7/1	3/0	8/0	19/13	3/1	0/2
3	0/1	0/0	0/4	0/2	0/1	0/5	0/3	0/0	0/2	0/2	0/6	0/26	0/3	82/108
4	6/0	8/43	0/1	2/1	5/1	1/0	ND/1	0/0	ND/12	ND/0	ND/0	ND	6/0	2/0
5	0/11	0/31	3/46	8/5	3/25	1/11	4/25	9/19	3/18	3/7	5/20	39/218	5/2	17/19
6	0/0	0/0	0/6	3/0	0/0	0/0	0/9	0/0	2/5	0/6	1/0	6/26	0/0	15/13
7	0/9	0/4	1/7	3/3	0/7	1/0	3/5	2/3	2/4	2/3	4/1	18/46	1/4	6/26
8	9/17	7/3	0/13	0/4	10/22	0/0	0/5	4/17	0/4	5/12	12/14	47/111	0/0	13/7
9	0/1	0/9	0/0	0/0	0/5	0/0	0/6	0/0	0/0	0/1	0/1	0/23	0/2	78/52
10	4/0	0/0	1/3	0/1	1/0	0/0	4/10	6/0	0/5	5/0	4/12	25/31	8/4	13/13
11	7/13	16/16	0/7	0/6	0/27	0/9	5/8	2/2	0/4	11/1	9/6	50/99	8/3	23/4
12	5/0	4/6	4/2	0/4	4/19	2/4	1/1	0/2	0/2	0/6	0/0	20/46	0/0	45/22
13	0/0	1/4	1/1	0/0	1/0	0/12	1/2	0/0	0/2	0/0	2/0	6/21	1/3	24/23
14	4/1	1/2	3/2	12/8	5/6	6/ND	3/ND	19/ND	5/ND	0/0	16/13	ND	2/2	34/7
15	1/2	2/4	0/0	2/1	4/1	1/1	0/2	1/5	0/5	1/0	4/3	16/24	0/0	0/3
16	0/0	1/0	1/2	4/0	1/1	0/2	0/0	2/1	1/0	1/0	5/0	16/6	1/0	32/23
17	1/13	0/11	1/11	0/2	2/4	0/3	6/13	1/10	7/4	ND/9	2/15	ND	ND/8	167/517
18	2/0	5/4	0/3	5/3	3/2	2/0	2/6	2/1	3/2	3/2	2/0	29/23	2/2	33/14
19	0/0	1/2	0/1	0/0	0/0	0/0	0/0	0/0	0/2	0/2	0/0	1/7	1/0	13/14
20	0/3	0/0	4/31	2/0	0/0	7/19	24/35	7/6	6/2	0/1	12/21	62/118	8/0	9/10
21	1/1	3/0	0/3	1/3	1/0	4/2	0/4	3/0	1/8	8/0	5/0	27/21	7/0	61/47
22	6/6	2/0	0/0	0/5	0/0	2/0	5/0	3/6	0/0	0/0	0/0	18/17	6/0	3/3
23	2/1	14/11	2/0	0/1	0/29	5/0	2/0	5/24	2/0	2/0	1/0	35/66	1/1	3/0
24	5/6	8/2	3/6	0/0	0/0	5/3	9/10	0/7	2/0	5/0	0/9	37/43	0/0	0/7
25	0/2	1/3	0/12	2/8	0/5	7/10	12/1	0/3	0/1	0/0	30/14	52/59	2/1	1/18
26	0/0	10/0	3/4	0/5	1/4	1/1	17/24	4/29	23/29	0/23	1/3	60/122	0/0	119/128
27	2/0	4/0	1/4	4/0	2/0	4/2	0/7	1/9	0/5	24/17	9/33	51/77	3/11	84/510
28	0/22	4/0	0/1	0/0	6/0	0/0	0/0	0/0	0/4	0/0	12/10	22/37	0/0	3/0
29	0/1	0/1	0/0	0/0	0/0	0/0	2/2	0/5	0/1	1/0	0/0	3/10	ND/0	9/4
30	0/0	0/0	0/0	0/0	4/12	0/0	0/1	1/10	6/4	0/0	0/10	11/37	8/1	316/ND
31	7/4	14/9	3/5	0/0	6/14	0/0	5/13	2/4	6/4	6/0	7/14	56/67	2/0	385/434
32	7/12	0/0	0/0	2/0	3/0	0/27	7/17	0/0	1/0	15/14	9/9	44/79	8/4	18/24
33	0/0	5/0	10/10	0/0	0/0	0/101	0/0	0/0	0/0	0/1	0/21	15/133	0/0	0/0
34	0/6	2/139	6/12	13/11	8/23	21/19	6/0	2/27	0/1	4/0	27/19	89/257	1/0	10/15
35	0/18	0/10	8/39	0/53	0/0	12/19	8/23	28/28	11/24	0/0	0/0	67/214	7/4	38/29
36	1/4	0/9	0/3	0/0	1/4	2/0	1/1	0/2	0/0	0/0	0/1	5/24	0/0	0/1
37	0/4	0/0	1/1	2/0	1/0	2/0	1/0	0/0	0/0	ND/0	ND/0	ND	ND/1	0/0
38	0/4	0/2	0/12	4/0	0/0	2/0	1/11	6/0	17/15	1/7	2/0	33/51	6/0	7/7
39	2/0	0/0	0/0	0/0	1/0	6/18	0/0	2/0	0/0	0/0	2/0	13/18	0/0	1/1
40	3/2	10/6	1/2	3/2	2/0	1/1	3/14	3/15	4/3	4/0	2/0	36/45	1/0	9/0
41	0/28	0/18	0/5	0/3	0/10	0/2	9/6	0/9	0/16	0/10	0/0	9/107	9/0	32/5
42	1/0	3/0	0/0	3/0	2/13	0/0	0/0	1/0	2/0	2/0	6/1	20/14	2/0	14/5
43	3/21	2/32	4/8	3/49	4/18	1/0	2/9	1/4	10/3	0/0	0/0	30/144	5/0	5/1
44	0/1	0/0	0/0	0/0	0/0	3/7	4/3	0/4	0/0	0/1	0/0	7/16	4/0	8/7
45	2/13	5/7	0/8	8/19	7/6	0/0	ND/23	0/5	ND/1	ND/5	ND/10	ND	7/6	14/9
46	0/0	0/0	0/0	0/0	0/3	0/10	0/11	0/2	ND/2	ND/ND	ND/13	ND	ND/0	7/15
47	5/14	8/7	3/4	6/2	5/14	1/0	7/6	2/0	8/5	5/0	2/8	52/60	7/12	4/6
48	0/0	0/2	0/0	2/0	0/0	0/0	0/0	0/1	0/2	0/0	0/4	2/9	0/0	121/60
49	1/0	3/0	7/10	4/0	3/3	1/0	0/8	0/0	0/5	5/4	0/0	24/30	0/0	22/71
50	1/5	0/1	5/1	ND/1	0/1	0/1	3/2	1/0	0/0	ND/0	0/0	ND	ND/1	5/3
51	0/1	9/2	0/57	1/7	1/0	0/2	0/12	1/1	1/4	1/3	1/0	15/89	2/0	38/50
52	3/2	1/0	0/0	1/0	1/0	0/7	3/2	1/2	9/8	0/2	1/4	20/27	0/4	1/8
53	4/0	6/17	2/0	0/0	8/2	1/2	9/0	6/4	6/2	5/0	17/10	64/37	9/0	1/0
54	3/1	3/0	11/19	6/10	2/5	15/18	11/26	11/11	16/10	12/23	14/19	104/142	25/1	97/276
55	1/9	2/3	25/15	6/0	21/15	0/9	36/18	42/26	11/14	5/0	18/15	167/124	8/0	119/94
56	0/0	0/9	0/0	0/0	0/0	0/3	0/0	13/4	2/0	0/0	0/0	15/16	1/0	47/16
57	0/7	8/11	0/2	0/0	3/7	7/0	5/10	4/2	9/11	3/0	0/0	39/50	6/0	25/28
58	0/5	0/10	4/13	8/7	0/6	7/6	9/20	4/14	14/12	9/5	7/4	62/102	1/6	48/47
59	5/0	7/2	3/6	18/4	0/0	3/0	0/10	6/0	8/0	77/0	12/3	139/25	5/0	64/61
60	0/53	0/12	7/13	0/12	1/102	0/0	16/19	6/3	5/18	0/0	4/18	39/250	6/0	22/21
61	2/27	13/14	0/15	24/28	5/0	7/0	6/25	14/18	11/15	3/19	2/23	87/184	0/0	23/2
62	0/0	0/17	9/0	0/0	13/0	4/0	10/0	12/0	7/0	9/0	4/0	68/17	5/0	139/48
63	0/4	0/0	0/3	0/0	4/0	0/0	0/3	0/0	0/0	4/0	0/0	8/10	ND/ND	ND/ND
64	3/0	11/17	3/99	4/0	4/11	2/0	5/0	2/0	12/7	3/2	3/0	52/136	5/0	22/30
65	9/8	3/4	0/0	0/0	4/4	8/13	0/0	9/1	7/0	0/0	1/0	41/30	8/0	107/55
66	0/0	0/0	0/0	0/0	0/0	0/0	0/1	0/0	0/1	0/0	0/0	0/2	0/1	0/1
67	0/14	5/27	0/6	0/9	0/8	ND/15	ND/26	ND/19	ND/19	ND/20	ND/14	ND	1/5	96/30
68	5/5	7/13	6/5	0/0	0/10	0/5	32/26	0/5	5/3	0/7	4/11	59/90	0/5	263/623
69	3/0	0/19	9/5	2/3	5/16	9/10	17/34	8/4	0/16	18/12	11/45	82/164	4/0	32/47
Response frequency	43	11	14	12	5	16	7	16	9	5	4	11	24	1	8
(%)	62.3	15.9	20.3	17.4	7.4	23.2	10.4	24.6	13.4	7.8	6.5	17.2	39.3	1.6	11.9

Fig. 1. Enhancement of TAA-derived peptide-specific T cell responses after RFA. The magnitude of TAA-specific T cell responses determined by the frequency of T cells responsive to each peptide before (the number of left side) and after (the number of right side) RFA and proportion of the patients with a significant increase are shown. Results with a significant increase are shown in gray boxes. The box numbers show the patients with a significant increase in TAA-specific T cell responses. The T cell responses were examined by IFN-γ ELISPOT assay. The results of ELISPOT assay are shown as a specific spot, which was determined by subtracting the number of spots in the absence of an antigen from the number in its presence. The increase was considered significant if more than or equal to 10 specific spots per 300,000 PBMCs were detected and if the number of spots after RFA was at least two-fold that before RFA. The patient characteristics are described in Table 1 and the peptide sequences are listed in Table 2.

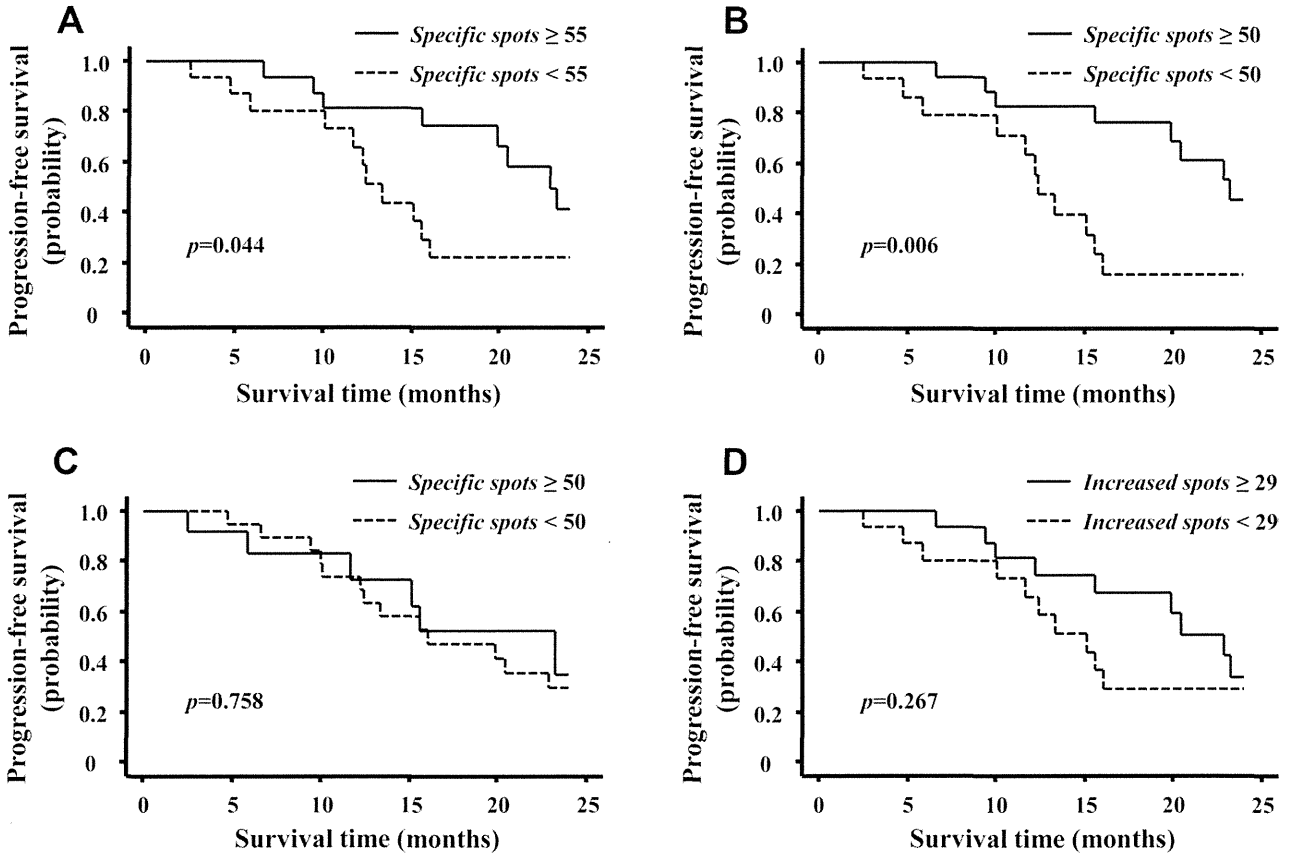

Fig. 2. Kaplan-Meier curves of HCC recurrence-free survival. (A) Kaplan-Meier curves indicating the relationship between month after RFA and HCC recurrence-free survival rate were grouped by the median number of TAA-specific T cells detected by IFN-γ ELISPOT assay after RFA. (B) The difference between the groups was emphasized when 50 spots were defined as highly specific spots. (C) Kaplan-Meier curves indicating the relationship between month after RFA and HCC recurrence-free survival rate were grouped by the number of TAA-specific T cells detected by IFN-γ ELISPOT assay before RFA. (D) Kaplan-Meier curves indicating the relationship between month after RFA and HCC recurrence-free survival rate were grouped by the median increased number of TAA-specific T cells after RFA.

When univariate analysis of prognostic factors for HCC recurrence-free survival was performed, γ-glutamyltransferase (<30), AFP (<400), Okuda stage,[1] and number of TAA-specific T cells after RFA (≥50) were detected as factors that decrease HCC recurrence rate after RFA (Table 3). When multivariate analysis including these three factors was performed, only the number of TAA-specific T cells after RFA (≥50) was found to be a factor that decreases HCC recurrence rate after RFA.

Analysis of the Factors that Affect the Number of TAA-Specific T Cells After RFA. To identify the factors that affect the number of TAA-specific T cells after RFA, we analyzed clinical parameters of patients and the frequency of $CD14^+HLA\text{-}DR^{-/low}$ MDSCs after HCC treatment. We could not find any clinical parameters correlated with the number of TAA-specific T cells after RFA.

The frequency of $CD14^+HLA\text{-}DR^{-/low}$ MDSCs after RFA showed various levels and depended on the patient (Fig. 3A,B). The frequency decreased significantly after RFA ($P = 0.022$) except in three patients (Fig. 3B) and correlated inversely with the number of TAA-specific T cells after RFA, but not with that of CMV-specific T cells (Fig. 3C).

Phenotypic Analysis of TAA-Specific T Cells Before and After RFA. Next, we examined the naïve/effector/memory phenotype of increased TAA-specific T cells after RFA using a tetramer assay. The memory phenotype was investigated by the criterion of CD45RA/CCR7 expression.[17] In tetramer analysis, the frequency of TAA-derived peptide-specific $CD8^+$ T cells before RFA was 0.00%-0.03% of $CD8^+$ cells (Fig. 4A). On the other hand, the frequency was increased after RFA in 10/12 (83.3%) patients, and the range was 0.00%-0.10% of $CD8^+$ cells. The frequency of $CD45RA^-/CCR7^+$ (central memory), $CD45RA^-/CCR7^-$ (effector memory), and $CD45RA^+/CCR7^-$ (effector) T cells in tetramer-positive cells depended on the patients, and the ratio of these cells changed after RFA (Fig. 4B). The frequency of tetramer-positive cells with $CD45RA^-/CCR7^+$ and $CD45RA^-/CCR7^-$ in $CD8^+$ cells was increased in 6/7 (85.7%) and

Table 3. Univariate and Multivariate Analysis of Prognostic Factors for Tumor-Free Survival

Variable	*P* Univariate Analysis	*P* Multivariate Analysis	HR (95% CI)
Age, <65/≥65 years	0.582		
Platelet count, <10/≥10 × 10^4/μL	0.570		
AST, <40≥40 IU/L	0.298		
ALT, <40≥40 IU/L	0.628		
γ-GTP, <30≥30 IU/L	0.010	0.223	2.408 (0.586-9.898)
Albumin, <3.5≥3.5 g/dL	0.588		
Total bilirubin, <1≥1 mg/dL	0.386		
Prothrombin time, <60%/≥60%	0.282		
DCP, <100/≥100 mAU/mL	0.630		
AFP, <400/≥400 ng/mL	0.008	0.056	0.216 (0.045-1.039)
L3, <10%/≥10%	0.100		
Child-Pugh score, A/B	0.260		
Tumor diameter, <2/≥2 cm	0.706		
Tumor multiplicity, solitary/multiple	0.686		
Okuda stage, 1/2	0.043	0.103	5.828 (0.698-48.630)
BCLC stage, A/BC	0.190		
CLIP score, 0,1/2,3	0.703		
HCV antibody, −/+	0.080		
No. of TAA-specific T cells before RFA, <50/≥50*	0.740		
Number of TAA-specific T cells after RFA, <50/≥50*	0.006	0.024	4.054 (1.203-13.664)

Abbreviations: ALT, alanine aminotransferase; AST, aspartate aminotransferase; BCLC, Barcelona Clinic Liver Cancer; CLIP, Cancer of the Liver Italian Program; DCP, des- γ-carboxy prothrombin γ-GTP, γ-guanosine triphosphate.

*Number of TAA-specific T cells before and after RFA was calculated per 3 × 10^5 PBMCs.

6/7 (85.7%) patients, respectively, whose samples were available for the assay before and after RFA. Interestingly, the tetramer-positive cells with $CD45RA^-/CCR7^+$ were newly induced after RFA in 5/7 (71.4%) patients.

Kinetics of TAA-Specific T Cells Induced by RFA. Although the number of TAA-specific T cells was a predictive factor of a decrease of HCC recurrence rate after RFA (as shown in Fig. 2A), more than 50% of the patients with a high number of TAA-specific T cells showed HCC recurrence for 25 months after treatment. To identify the relationship between TAA-specific T cell responses and HCC recurrence more precisely, we examined the kinetics of TAA-specific T cells in 16 patients whose PBMCs were available for analysis at 24 weeks after RFA. The frequencies of TAA-derived peptide-specific T cells decreased in most of the peptides and patients at 24 weeks after RFA (Fig. 5). In the analysis of the total of each type of TAA-derived peptide-specific T cells, the frequency decreased in 14/16 (87.5%) patients analyzed, and most of them showed fewer than 50 specific spots per 3 × 10^5 PBMCs, with the exception of one patient. In contrast, the frequencies of CMV-derived peptide-specific T cells were maintained in most of the patients.

Discussion

In recent years, HCC-specific TAAs and their T cell epitopes have been identified, which has made analysis of immunological status in HCC patients possible and shown that TAA-specific T cell responses can be detected in peripheral blood.[11,18-20] The immunological analysis of HCC patients with RFA using 11 TAA-derived peptides in this study showed that the enhancement of TAA-specific T cell responses occurred in 62.3% of patients, the antigens and their epitope to which enhanced T cell responses occurred were diverse, and some of them were newly induced. The mechanism of enhancement of tumor-specific immune response by RFA is still unclear. den Brok et al.[5] showed that RFA created an antigen source for antitumor immunity by destruction of tumor cells using a mouse tumor model. The antigens used in this study have been reported to be located in the cell membrane (MRP3), cytoplasm (SART2 and AFP), and nucleus (hTERT and SART3).[21-24] The diversity of the target proteins of enhanced T cells suggests that the central mechanism of enhancement of tumor-specific immune response by RFA is due to tumor cell destruction, which supports the results mentioned previously.[5]

In the present study, we also showed that the number of TAA-specific T cells after RFA was associated with the HCC recurrence-free survival of patients. The univariate and multivariate analyses clearly showed it was a predictive factor for HCC recurrence after RFA. These results suggest that TAA-specific T cells induced by RFA contribute to protection from HCC recurrence, and additional immunological approaches should be applied to enhance the protective effect after treatment.

To understand the precise mechanism that RFA enhances TAA-specific T cell responses, we analyzed the factors that affected the number of TAA-specific T cells after RFA. Among the factors analyzed, the frequency of $CD14^+HLA\text{-}DR^{-/low}$ MDSCs after RFA was inversely correlated with the number of TAA-specific T cells, suggesting these MDSCs may have a negative effect on TAA-specific immune responses. Regarding the function of MDSCs in cancer patients, it has been reported that they inhibit T lymphocyte responses.[25] In HCC patients, it is reported that the frequency of $CD14^+HLA\text{-}DR^{-/low}$ MDSCs in